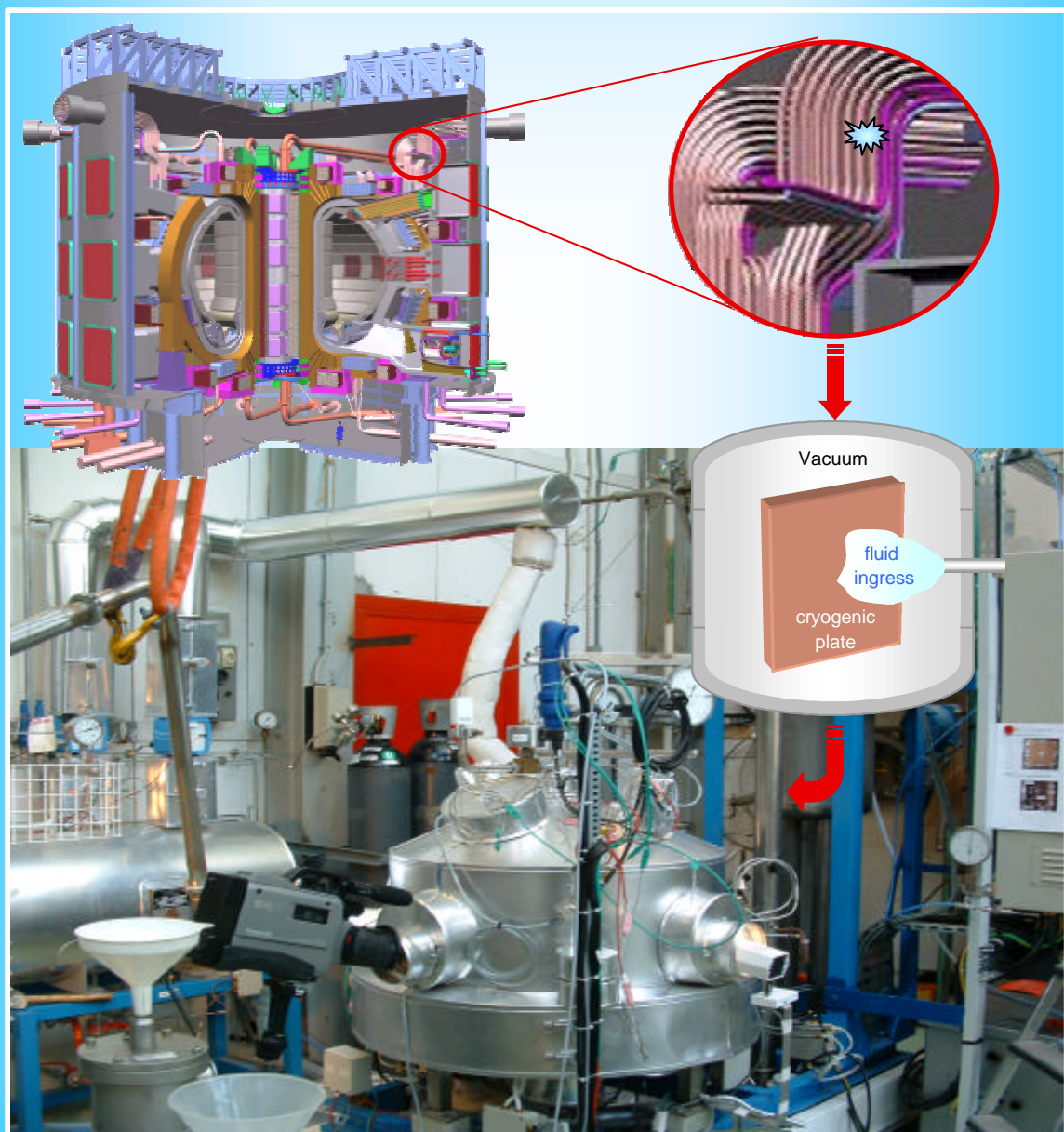


FUSION TECHNOLOGY

Annual Report of the Association EURATOM/CEA 2002

Compiled by : Ph. MAGAUD and F. Le VAGUERES



ASSOCIATION EURATOM/CEA
DSM/DRFC
CEA/CADARACHE
13108 Saint-Paul-Lez-Durance (France)

CONTENTS

INTRODUCTION	1
---------------------------	---

EFDA TECHNOLOGY PROGRAMME	3
----------------------------------------	---

Physics Integration

Heating and Current Drive

CEFDA01-645	Support to neutral beam physics and testing 1	5
CEFDA01-646	Support to neutral beam physics and testing 2	9
TW1-TPH-ICRANT	ICRF antenna and vacuum transmission line development - Design and manufacturing of a cw ICRF high power test rig and testing of next step antenna prototype components	13

Remote Participation

CEFDA01-647	Support to remote participation in EFDA - RP technical infrastructure assistant	15
TW1-TP/RPINF	Development of remote participation infrastructure - Local support to remote participation in the CEA-DRFC	17

Vessel/In-Vessel

Vessel/Blanket

T216-GB8	Small scale testing of FW/BS modules	21
TW0-T420/06	Fabrication of a first wall panel with HIPped beryllium armor	23
TW0-T420/08	Development of HIP fabrication technique	25
TW0-T508/04	Development of Be/CuCrZr HIPping technique	29
TW0-T508/05	Development of Be/CuCrZr brazing technique	31
TW1-TVV-HIP	Improvement of HIP fabrication techniques	33
TW1-TVV-LWELD	VV intersector joining - Further development of high power Nd-YAG laser welding with multipass filler wire	39
TW1-TVV-ONE	Optimisation of one step SS/SS and SS/CuCrZr HIP joints for retainment of CuCrZr properties	43
TW2-TVB-HYDCON	Procurement and testing of cutting/welding and inspection tool for the blanket module hydraulic connector	47

TW2-TVV-DISMIT	Evaluation of methods for the mitigation of welding distortions and residual stresses in thick section welding	51
TW2-TVV-UTINSP	Further development of ultrasonic inspection process	53

Plasma Facing Components

CEFDA99-501	Critical heat flux testing and fatigue testing of CFC monoblocks - 200 kW electron beam gun test	57
CEFDA01-581	Critical heat flux testing of hypervaportrons - 200 kW electron beam gun test	61
CEFDA02-583	Destructive examination of primary first wall panels and mock-ups	65
DV4.3	Optimisation and manufacture of HHF components - Study of flat tile cascade failure possibility for high heat flux components	67
TW0-T438-01	Development and testing of time resolved erosion detecting techniques	71
TW1-TVP-CFC1	Neutron effects on dimensional stability and thermal properties of CFCs	73

Remote Handling

T329-5	In-vessel RH dexterous operations	77
TW0-DTP/1.2 TW0-DTP/1.4 TW1-TVA-IVP TW2-TVR-IVP	In-Vessel Penetrator (IVP) - Prototypical manipulator for access through IVVS penetrations	81
TW1-TVA-BTS	Bore Tool Systems (BTS) - Carrier and bore tools for 4" bent pipes	85
TW1-TVA-MANIP	In-vessel dexterous manipulator	89
TW1-TVA-RADTOL	Radiation tolerance assessment of remote handling components	91

Magnet Structure

CEFDA00-541	Magnet design on PF and correction coils: Conceptual design and analysis	97
M40	Design work on magnet R&D	101
M50	Conductor R&D - Development of NbTi conductors for ITER PF coils	103
TW0-T400-1	CSMC and TFMC installation and test	107
TW1-TMC-CODES	Design and interpretation codes - Determination of thermohydraulic properties of cable-in-conduit conductors with a central channel	109
TW1-TMC-SCABLE	Cable and conductor characterisation - Determination of critical properties and losses of superconducting strands and cables for fusion application	111
TW1-TMS-PFCITE	Poloidal Field Conductor Insert (PFCI)	113
TW2-TMST-TOSKA	TFMC testing with the LCT coil	115

Tritium Breeding and Materials

Breeding Blanket

Water Cooled Lithium Lead (WCLL) blanket

TW1-TTBA-001-D01	TBM adaptation to next step machine	119
TW1-TTBA-001-D03	TBM adaptation to next step machine - Adaptation of mechanical performances to ITER specifications	123
TW2-TTBA-001a-D04	Completion of design activities on WCLL and final report	129
TTBA-2.2	Blanket manufacturing techniques - Solid HIP demonstrator for fabrication and coating	133
TW1-TTBA-002-D05	Blanket manufacturing techniques - Integrated mixed-powder HIP fabrication route for TBM with DWT	137
TW2-TTBA-002a-D02	Crack propagation test and interpretation on unirradiated DWT	141
TW1-TTBA-005-D02	Safety and licensing: Pb-17Li/water interactions	145

Helium Cooled Pebble Bed (HCPB) blanket

TW1-TTBB-002-D02	Blanket manufacturing techniques – Mock-up of FW manufactured with alternative reduced cost fabrication technique	149
TW2-TTBB-002a-D04	Blanket manufacturing techniques - Assessment of first wall fabrication techniques and first wall to stiffening plates joining techniques	151
TW2-TTBB-005a-D03	Development of ceramic breeder pebble beds - Characterization of Li_2TiO_3 pebbles	155
TW2-TTBB-005a-D04	Development of ceramic breeder pebble beds - Mastering and optimising of process parameters for the preparation of Li_2TiO_3 powder and for the fabrication of Li_2TiO_3 pebbles	159

Helium Cooled Lithium Lead (HCLL) blanket

TW2-TTBC-001-D01	Helium-cooled lithium lead - TBM design, integration and analysis - Blanket system design and analysis - Integration and testing in ITER	163
------------------	------------------------------------------------------------------------------------------------------------------------------------------------	-----

Structural materials development

Reduced Activation Ferritic Martensitic (RAFM) steels

TW1-TTMS-001-D02	RAFM steels - Irradiation performance -	
TW2-TTMS-001a-D02	Neutron irradiation to 35 dpa at 325°C	167
TW2-TTMS-002a-D04	RAFM steels - Metallurgical and mechanical characterization of Eurofer 97 Thermal ageing behaviour	171
TW2-TTMS-002a-D17	RAFM steels - Tensile and impact test on Eurofer weldments	175
TW2-TTMS-002a-D18	RAFM steels - Tensile and charpy properties of Eurofer powder HIP material	179

TW1-TTMS-003-D12	SCC behaviour of Eurofer 97 in water with additives - Materials compatibility in fusion environments	183
TW2-TTMS-004a-D01	RAFM steels - Eurofer: Powder HIP processing and specification	185
TW2-TTMS-004a-D04	RAFM steels - Eurofer: Fusion welds of structural parts (homogenous welding)	189
TW2-TTMS-004a-D05	RAFM steels - Eurofer: Dissimilar welds development	193
TW2-TTMS-004a-D08	RAFM steels - Powder HIP materials joining	197
TW2-TTMS-004b-D01	RAFM steels - Tubing process qualification: advanced process development and testing for the production of TBM's cooling channels	201
TW2-TTMS-005a-D02	RAFM steels - Rules for design and inspection - DISD appendix A for RAFM steel, intermediate appendix A for the Eurofer steel	205
TW2-TTMS-005a-D05	RAFM steels - Rules for design, fabrication and inspection - Data collection and data base maintenance, update data base for Eurofer steel	209
TW2-TTMS-006a-D01	RAFM steels - ODS processing and qualification	211
TW2-TTMS-006a-D11 TW2-TTMS-006a-D12	ODS/Eurofer HIP joining feasibility solid/solid and solid/powder	215

Advanced materials

TW2-TTMA-001a-D06	Compatibility of SiC/SiC with flowing liquid Pb-17Li	219
TW2-TTMA-002a-D04	Feasibility of joining W onto Cu and RAFM steel	223

Neutron source

TTMI-001-D1	IFMIF, accelerator facility - Electron Cyclotron Resonance (ECR) source	225
TTMI-001-D4	IFMIF, accelerator facility - 4 vanes Radio Frequency Quadrupole (RFQ) design	227
TTMI-001-D5	IFMIF, accelerator facility - Radio frequency tube	231
TTMI-001-D6	IFMIF, accelerator facility - Drift Tube Linac (DTL) design	235
TTMI-001-D9	IFMIF, accelerator facility - Diagnostics	239

Safety and Environment

SEA5-31	Validation of computer codes and models	243
TW1-TSS-SEA5	Validation of computer codes and models	245
TW0-SEA3.5 TW1-TSS-SEA3.5	In-vessel hydrogen deflagration/detonation analysis	247
TW1-TSS-SERF2	Tritium releases and long term impacts	249
TW1-TSW-002	Waste and decommissioning strategy	253

System Studies

Power Plant Conceptual Studies (PPCS)

TW1-TRP-PPCS1-D04	Model A (WCLL): Consistency with the PPCS GDRD	255
TW1-TRP-PPCS1-D10	Model A (WCLL): Mechanical analysis design integration	257
TW1-TRP-PPCS5-D03	Environmental assessment: Waste management strategy	261
TW2-TRP-PPCS10-D07	Model D (SCLL): Adaptation of SiC _f /SiC - Pb-17Li divertor concept to the new advanced reactor models	265
TW2-TRP-PPCS11-D01	Model A (WCLL): Study of a high temperature water cooled divertor	269
TW2-TRP-PPCS12-D06	Model D (SCLL): Shield and vacuum vessel design	273
TW2-TRP-PPCS13-D06	Model D (SCLL): Mechanical and thermo-mechanical analysis of the SCLL blanket	277
TW2-TRP-PPCS13-D07	Model D (SCLL) : Design integration (including divertor system)	281

Socio-economic studies

CEFDA01-630 TW1-TRE-FPOA	Fusion and the public opinion: Public acceptance of the siting of ITER at Cadarache	287
TW1-TRE-ECFA-D01	Externalities of fusion: Comparison of fusion external costs with advanced nuclear fission reactors	291
TW1-TRE-ECFA-D02	Externalities of fusion accident: Sensitivity analysis on plant model and site location	295

JET Technology

Physics Integration

Diagnostics

CEFDA01-624	Diagnostics enhancement - IR viewing project management and implementation	299
-------------	-------------------------------------------------------------------------------------	-----

Vessel/In-Vessel

Plasma Facing Components

JET-EP-Div	JET EP divertor project	303
JW0-FT-3.1	Internal PFC components behaviour and modelling	305

Remote Handling

CEFDA01-609	Lessons learned from JET maintenance and remote handling operation	307
-------------	--------------------------------------------------------------------------	-----

Safety and Environment

JW0-FT-2.5	Tritium processes and waste management - Dedicated procedures for the detritiation of selected materials	311
------------	-------------------------------------------------------------------------------------------------------------------	-----

UNDERLYING TECHNOLOGY PROGRAMME	315
----------------------------------------------	------------

Physics Integration

Diagnostics

UT-PE-HFW	Transparent polycrystalline windows	317
-----------	-------------------------------------------	-----

Vessel/In-Vessel

Plasma Facing Components

UT-VIV/PFC-TMM	Thermo-Mechanical Models (TMM)	321
UT-VIV/PFC-W/Coat	Development of thick W CVD coatings for divertor high heat flux components	325

Remote Handling

UT-VIV/AM-Actuators	Remote handling techniques - Advanced technologies for high performances actuators	327
UT-VIV/AM-ECIr	Remote handling techniques - Radiation tolerance assessment of electronic components from specific industrial technologies for remote handling and process instrumentation	329
UT-VIV/AM-HMI	Remote handling techniques - Graphical programming for remote handling techniques	335
UT-VIV/AM-Hydro	Remote handling techniques - Technologies and control for remote handling systems	339

Tritium Breeding and Materials

Breeding Blanket

UT-TBM/BB-BNI	Blanket neutronic instrumentation	343
UT-TBM/BB-He	Helium components technology - Problems and outlines of solutions	347
UT-TBM/MAT-LM/MAG	Liquid metal corrosion under magnetic field	349
UT-TBM/MAT-LM/Refrac	Compatibility of refractory materials with liquid alloys	353
UT-TBM/MAT-LM/SiC	Compatibility of SiC _f /SiC composites with liquid Pb-17Li	357
UT-TBM/MAT-LM/WET	Wetting of materials by liquid metals	361

Materials development

Structural materials

UT-TBM/MAT-BIM	Dissimilar diffusion - Bonded joints - Mechanical testing	365
UT-TBM/MAT-HHFC/REFR	Review of refractory metals and alloys for application to high temperature components	369
UT-TBM/MAT-LAM/DES	Design of new reduced activation ferrito-martensitic steels for application at high temperature	371
UT-TBM/MAT-LAM/Mic	Influence of the martensite morphology on the plasticity behaviour of the Eurofer steel	375
UT-TBM/MAT-LAM2	Irradiated behaviour of Reduced Activation (RA) martensitic steels after neutron irradiation at 325°C	379
UT-TBM/MAT-LAM3	Microstructural investigation of Reduced Activation Ferritic Martensitic (RAFM) steels and Oxide Dispersion Strengthened (ODS) steels by Small Angle Neutron Scattering (SANS)	383
UT-TBM/MAT-Mod	Modelling of the resistance of the dislocation network to the combined effect of irradiation and stress - Secondary defects structure in an annealed 316L steel after a pulsed and a continuous irradiation - Interaction of pre-existent dislocations and point defects	387
UT-TBM/MAT-ODS	Development of forming and joining technologies for ODS steels	393

Fuel cycle

UT-TBM/FC-SP	Separation of the D/T mixture from helium in fusion reactors using superpermeable membranes - Superpermeable membranes resistant to sputtering - Proposal for superpermeable membrane practical application in fusion	397
--------------	-----------------------------------------------------------------------------------------------------------------------------------------------------------------------------------------------------------------------------------	-----

Safety and Environment

UT-S&E-LASER/DEC	Laser decontamination: Tritium removal	401
UT-S&E-Mitig	Evaluation and mitigation of the risk connected with air or water ingress	407

System studies

UT-SS-REL	Reliability/availability assessment - Integral approach to assess the availability of the fusion power reactor conceptual designs	409
-----------	--------------------------------------------------------------------------------------------------------------------------------------------	-----

<i>INERTIAL CONFINEMENT FUSION PROGRAMME</i>	413
-----------------------------------------------------------	------------

ICF01	Intense laser and particle beams dynamics for ICF applications	415
ICF03	Laser-matter interaction at relativistic intensities and fast igniter studies	419
ICF04	EU collaborative experiment on the fast igniter concept	423

ICF-KiT-PRC	Overview on power reactor concepts	425
ICF-XUV-Diag	Dense plasma diagnostics using high order harmonics generation	427

<i>APPENDIX 1 : Directions contribution to the fusion programme</i>	431
---------------------------------------------------------------------------	-----

<i>APPENDIX 2 : Allocations of tasks</i>	435
------------------------------------------------	-----

<i>APPENDIX 3 : Reports and publications</i>	441
----------------------------------------------------	-----

<i>APPENDIX 4 : CEA tasks in alphabetical order</i>	451
-----------------------------------------------------------	-----

<i>APPENDIX 5 : CEA sites</i>	455
-------------------------------------	-----

Task Title: TBM ADAPTATION TO NEXT STEP MACHINE

INTRODUCTION

The water-cooled lithium-lead (WCLL) breeding blanket [1] is based on the principle of using the well-established PWR-technology for the power conversion cycle (water coolant at 15.5 MPa, outlet temperature 325°C) and of slowly circulating a liquid tritium breeder, the PbLi, for extracting the tritium outside the reactor. A WCLL Test Blanket Module (TBM) to be tested in ITER is under development for few years, whose main body is quite similar to the equatorial part of an inboard segment of the corresponding DEMO blanket.

It is expected to use all technologies required for that concept: martensitic steel as structural material, liquid PbLi as breeder and neutron multiplier, and light water at typical PWR conditions as coolant.

Beside the optimization of the neutronic, thermal and mechanical behaviour of the TBM (previously reported in the 2001 report [2]), the integration of the related EU R&D results and the definition of the future R&D needs is also a key part of the activity.

In that sense, a synthesis of the main 2001-02 R&D results obtained on the WCLL EU programme has been completed in 2002.

In particular, key results obtained in the field have been reported and their impact on the blanket design analyzed.

2002 ACTIVITIES

The main WCLL R&D results obtained within the EU workprogramme, in particular in the field of blanket manufacturing, coating (tritium control) qualification and PbLi/water accidental interaction, have been synthesized for integration in the TBM design and fabrication sequence.

They are summarized hereafter. Detailed references issued within the EU programme can be found in the activity report.

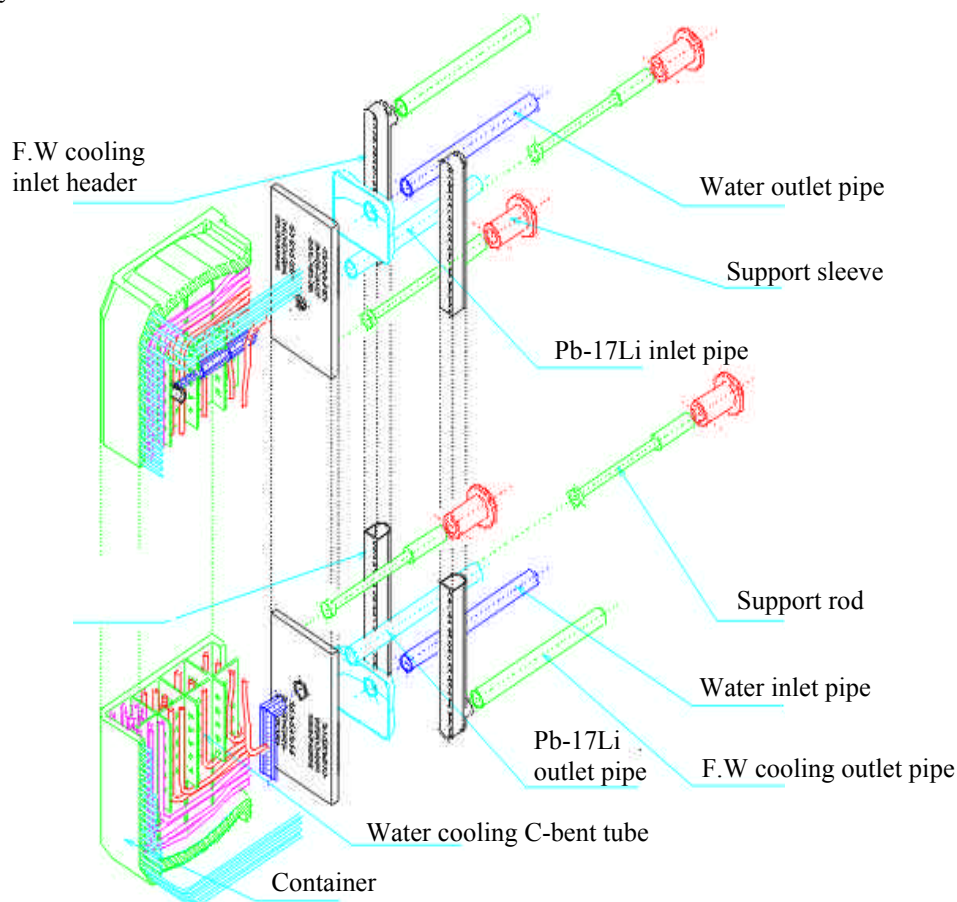


Figure 1 : 3D view of the WCLL TBM

BLANKET MANUFACTURING

Double-Wall Tubes (DWT)

Fabrication and qualification of Double Wall Tubes (DWT), used for reducing the probability of pressurized water leakage into the liquid PbLi, is a key part of the Blanket manufacturing R&D.

R&D has demonstrated that DWT (consisting in two concentric Eurofer tubes – diameters 11/13.4 and 13.6/16.5 mm – separated with a 0.1 mm Cu interlayer) can be fabricated by diffusion bonding through a HIP process (980°C, 100 MPa for 2 hours). The Cu layer is deposited before HIP on the inner tube by electroplating. Up to now, a 0.1-0.2 µm Ni layer was applied before Cu deposition.

Very recent optimization allowed to define suitable experimental conditions that provide Cu coating adherence without any Ni sub-layer. R&D has also shown that removing the initial gap between the inner and outer tubes by mechanical expansion before HIPing may reduce significantly the final DWT outer diameter variation after HIPing (from 0.4 mm variation without pre-expansion to 0.05 mm).

It has been also demonstrated that DWT bending after HIP provide better accuracy performances rather than bending before HIP. HIPed DWT have been bent up to a curvature radius near to the minimum specification (50 mm) and no visible damage was observed at the Eurofer/Cu interface. Although an ovalisation of the channel cross section is observed, a total surface decrease of only 4 % has been observed which within the range of the specification (< 15 %).

The thermal cycling qualification of the Eurofer/Cu/Eurofer joint of DWT was initiated in DIADemo with straight DWT (T91 instead of Eurofer) and continued on a curved Eurofer DWT. More than 3000 WCLL relevant thermal cycles were successfully applied and then, a leak appeared during endurance test. Post-test examination was performed on the DWT sample. Despite high temperature and high pressure He test, no evidence of tube damage could be found. Further examination or test will be necessary, but a leak somewhere else in the test section can now not be precluded.

Crack propagation test on small-scale Eurofer sample submitted to 4-point bending cycles have been initiated and shall demonstrate the ability of DWT to stop – or at least deviate – cracks occurring on one of the tubes to the other. Encouraging screening tests have been carried-out in that sense.

First Wall (FW)

The FW consists in a 26 mm thick Eurofer cooled by internal channels. As for the breeder zone DWT, a thin 0.1 mm Cu interlayer is foreseen between the steel cooling tube and the steel structure.

Several fabrication options have been examined and it appears that the full solid-plates HIPing process may present drawbacks (local variation of the Cu thickness at the plate junction) that could be by-passed using a mixed powder/solid process. In this case, Eurofer (powder) / Eurofer (plate) joint presents similar properties compared to solid/solid joint.

However, it has been noted that Eurofer grains deformed locally the soft Cu during HIPing. This could be optimized in the future by reducing the HIP pressure during the heating up phase. Other acceptable solutions could be to decrease the Eurofer grain size or slightly increase the Cu thickness up to ~0.2 mm which would have limited impact on thermal behaviour of the DWT.

An optimization of the groove design where tubes are inserted before HIPing has been carried out and a more complex mixed powder/solid demonstrator shall be fabricated for further validation.

COATING (TRITIUM CONTROL) QUALIFICATION

Up to now, the use of permeation barriers in the WCLL DEMO Blanket was imposed by the previously accepted tritium permeation limit of 1 g/d at a concentration level of 1 Ci/kg of T in the primary cooling water.

In the last few years, different studies were performed in parallel to minimize the development risk: on one hand, coatings were optimized and tested, and on the other hand, solutions were investigated on how to minimize the requirements of these coatings and thus to minimize the consequences of unsuccessful R&D.

It has been demonstrated in 2000-2001 that the WCLL concept can tolerate higher tritium permeation into the primary coolant (of the order of 10-20 g/d, thus assuming permeation barriers with low performance requirements) without prohibitive effects on safety and incremental capital and operative costs of the WDS (Water Detr^{it}iation System).

This can be achieved by increasing the tritium concentration in the coolant to some 8 Ci/kg which keeps the cost for tritium extraction low while no safety concern is raised (classical LOCA release scenario) due to the increase in inventory.

However, further R&D on permeation barriers was maintained because: i) safety studies need confirmation, ii) permeation barriers may remain a cost reduction factor which should not be precluded, iii) the potential benefits of a coating to minimize corrosion and activated corrosion product transport (worker and occupational safety) have to be further assessed.

Tritium Permeation Barriers (TPB) – consisting of Al rich coatings, which forms Al₂O₃ at their surface – have been further tested in 2001 in the VIVALDI facility in gas and PbLi phases. The VIVALDI apparatus was successfully developed to eliminate parasitic effects in such experiments.

Eurofer samples coated by CVD (Chemical Vapor Deposition) and HD (Hot Dipping) were tested in 2001 and it appeared that the measured Permeation Reduction Factor (PRF) were lower than those found previously with MANET coated samples. This general trend is not related to the choice of coating or substrate but has been explained by the quality of coatings probably due to an insufficient surface preparation (which is especially important with Eurofer products). Further experiments on new samples has been launched and shall confirmed this conclusion.

Preliminary in-pile testing of TPB within the EXOTIC-8/10 experiment in HFR (T91 tubes – CVD) has been extended to about 2.5 dpa (steel) and no deterioration of the PRF was observed.

PbLi/WATER ACCIDENTAL INTERACTION

Both experimental and numerical modelling R&D activities were launched in parallel in the past years. On one hand, experimental activities previously carried out within the BLAST campaign have been extended more recently with the LIFUS-5 tests. On the other hand, based on experimental results, the SIMMER-III numerical code is under validation and promising results have been obtained.

Significant experimental results have been obtained in 2001-02 with the continuation of the LIFUS-5 campaign (injection of pressurized water in PbLi). In particular, runs n.3 to n.5 reached relevant WCLL conditions and the maximum pressure in the reaction vessel never exceeded the injected water pressure (15.5 MPa) for which the TBM is designed under faulted conditions. Analysis of the different phases of the interaction and sensitivity to the counter pressure in the expansion vessel allowed to give recommendation for the TBM System design.

On the other hand, numerical modeling of the thermal interaction using the SIMMER-III code made some significant progress with, firstly, validation of the code on the simplified geometry BLAST experiment and, secondly with preliminary models of the more complex geometry experiment LIFUS-5. In particular, a 2D equivalent model has been developed and will be further validated and compared to last LIFUS experimental results. In case a 2D approach would be too limited, 3D capabilities should be implemented in the SIMMER-III code.

CONCLUSION

The R&D performed in the framework of the EFDA Technology 2001-02 workprogramme on the WCLL Breeding Blanket has reached major goals which have been synthesized and analyzed in the 2002 activity. Most of them have been already integrated in the detailed design and manufacturing sequence of the WCLL Test Blanket Module [2, 3]. Others, more recent, will be integrated later, but do not question, in any case, the feasibility or performances of the WCLL concept.

REFERENCES

- [1] L. Giancarli et al., Development of the EU water-cooled Pb-17Li blanket, Fusion Eng. and Design 39-40 (1998) 639-644.
- [2] Y. Poitevin et al., « Status of the design and testing programme of the WCLL Test Blanket Module for ITER-FEAT », CEA technical report SERMA/RT/01-3019/A, December 2001.
- [3] Y. Poitevin et al., « Fabrication sequence of the WCLL Test Blanket Module for ITER-FEAT », CEA technical report SERMA/RT/01-3020/A, January 2002.

REPORT

Y. Poitevin et al., “WCLL Blanket concept: synthesis of last R&D results and impact on the Test Blanket Module design”, CEA technical report, SERMA/RT/02-3061, December 2002.

TASK LEADER

Yves POITEVIN

DEN/DM2S/SERMA
CEA Saclay
91191 Gif-sur-Yvette Cedex, France

Tél. : 33 1 69 08 31 86
Fax : 33 1 69 08 99 35

E-mail : ypoitevin@cea.fr

Task Title: TBM ADAPTATION TO NEXT STEP MACHINE

Adaptation of mechanical performances to ITER specifications

INTRODUCTION

The objective of the deliverable was initially to assess innovative design solutions aiming at reducing the amount of steel in the WCLL Blanket and, by consequence, in the TBM in order to optimise their neutronic performance. This activity was then strongly linked to the shape and segmentation of WCLL Blankets.

Considering that Power Plant Conceptual Studies launched in 2001 were questioning the WCLL banana-shape of modules, it appeared more appropriate to delay this activity until the achievement of the PPCS studies. This would have allowed to perform the analysis on the basis of an updated and relevant module segmentation.

However due to the re-organization of the liquid breeder concept towards He cooling, it has been agreed to perform this activity in the frame of the new Helium Cooled Lithium Lead (HCLL) project, keeping the same initial objective to optimise the amount of steel in the blanket.

In that sense, internal accidental pressurization (in-box accidental He leaks) has been carefully analysed, since it appeared to be the leading issue for steel structure optimisation in a HCLL blanket module.

2002 ACTIVITIES

2002 activities focused on the assessment of the mechanical behaviour of the module box for an accidental internal pressure of 8 MPa (in-box He leaks). Parametric analyses have been performed on a model representative of a design based on the use of horizontal cooling plates reinforced by vertical plates [1].

The goal was to identify the expected stresses level, the maxima localizations and to optimise the amount of steel needed to reinforce the structure.

GEOMETRY MAIN DATA

Complete information on the HCLL blanket module can be found in [1]. Table 1 lists the main data used for the structure definition of the module. Some key dimensions (indicated as “*param*” in table 1) have been submitted to a parametric study around the reference value given in table 1, in order to point out some optimisation trends in the structure behaviour. The different studied cases can be found later in the document (table 3).

DESIGN CRITERIA AND MATERIAL DATA

The design criteria used in these analyses are based on documents [2] and [3]. Accidental pressurization of the blanket module is classified under faulted conditions, and the level D criteria are used (the possibility to return to service a component subjected to a loading limited by level D criteria is not guaranteed).

The Eurofer mechanical properties summarized in the table 2 have been used in the analyses [3]. The Young's modulus was considered constant, as its low variation range had no consequence on the results.

Table 1 : HCLL blanket module geometry main data (dimensions in mm)

MODULE INNER DIMENSIONS	
Radial depth	870
Poloidal length	2000
Toroidal length (<i>param.</i>)	4000
First wall (FW) / Side walls (SW)	
Channel section	16 x 16
Channel pitch	22
Channel direction	FW : toroidal; SW : radial
Inner & outer thicknesses	FW:5 & 4; SW:5 to 15 & 4
Cooling plates (CP)	
Pitch	44
Channel section	3 x 3
Channel pitch	5
Channel direction	radial
Overall thickness (<i>param.</i>)	5
Back plate (BP)	
Thickness	50
Vertical plates (VP)	
Equivalent thickness	6
Pitch (<i>param.</i>)	400
Module caps	
Thickness (<i>param.</i>)	40

Table 2 : Mechanical characteristics for Eurofer

Young's modulus at 350 °C (MPa)	200000	
Poisson's ratio	0.3	
min(0.7Su ; 2.4Sm)	T (°C)	MPa
	350	341
	400	324
	450	304
	500	278
	550	246

MODELLING

The whole analysis (pre-processing, calculations, post-processing) has been performed with the CASTEM computer code, developed at CEA/Saclay.

In order to avoid the modelling of the whole module, the analysis rely on two local three-dimensional models:

- a radial-toroidal slice (figure 1),
- a radial-poloidal slice (figure 2).

The models have been simplified in order to limit calculation time:

- Use of symmetry and repetition planes as cutting planes; in various cases, representing the whole length of the slices was too costly, and tests have shown that the models could be reduced to take into account only some stiffening plates, i.e. CP or VP, near the module boundaries, for the same results. Typically, for the radial-toroidal slice with VP, only the first four VP near the SW have been represented, and, for the radial-poloidal slice, only the first two CP near the cap have been represented. The cutting planes were then considered as symmetry planes.
- Simplified BP.
- Homogenized CP with equivalent orthotropic properties to take the cooling channels into account.
- Homogenized VP with assumed equivalent thickness, as the cooling channels distribution is not completely identified.

Several cases have been analysed for this study, corresponding to different design parameters. The table 3 gives the specific characteristics of each geometric case.

All the calculations have been made with linear formulations for the finite elements; a test with quadratic formulation has been performed to ensure that the resulting loss when using linear elements was acceptable. Mesh examples are given in figures 1 and 2.

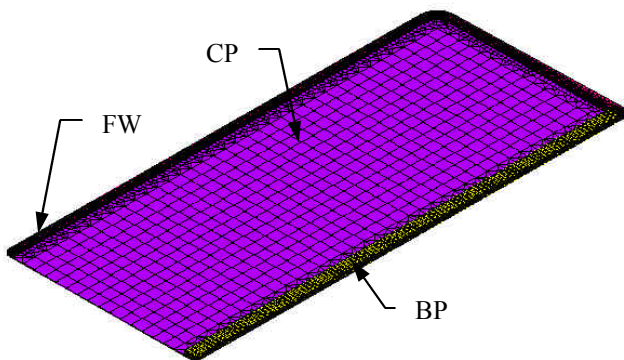


Figure 1 : RT01 model, mesh

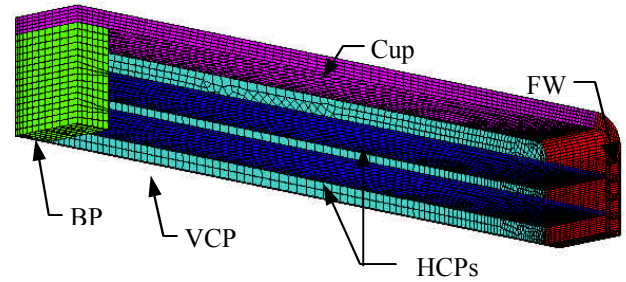


Figure 2 : RP01 model, mesh

For all the models, the boundary conditions were the followings:

- normal displacement locked for the symmetry planes;
- other cutting planes stay parallel to themselves; effects of pressure in enclosed volume (pressure on caps or SW) uniformly reported on these sections;
- one point fixed to avoid rigid body motion.

The only loading is due to internal pressure, assumed to be 8 MPa in all the cooling channels, and accidentally, in the module.

Table 3 : Characteristics and design parameters
of the studied cases

Model	Specific characteristics
RT01	Radial-toroidal slice without VP, CP welded on all edges
RT02	Radial-toroidal slice without VP, toroidal inner length 2 m, CP welded on all edges
RT03	Radial-toroidal slice with VP (200 mm pitch), CP welded on all edges
RT04	Radial-toroidal slice with VP (200 mm pitch), CP disconnected from BP
RT05	Radial-toroidal slice with VP (200 mm pitch), CP alternatively disconnected from BP or FW
RP01	Radial-poloidal slice with 200 mm pitch between VP, 20 mm thickness for caps
RP02	Radial-poloidal slice with 400 mm pitch between VP, 40 mm thickness for caps

ORTHOTROPIC EQUIVALENT PROPERTIES FOR CP

CPs (in reality featuring internal cooling channels [1]) have been represented as filled plates with orthotropic equivalent mechanical properties, so that the mesh is lighter and simple, and the 'global' displacements are respected on tension loads. These equivalent properties have been calculated using a local finite elements model of the CP.

For an isotropic Young's modulus of 200000 MPa (assumed to be constant, and with the "reference" dimensions of the channels, the values summarized in the table 4 were found:

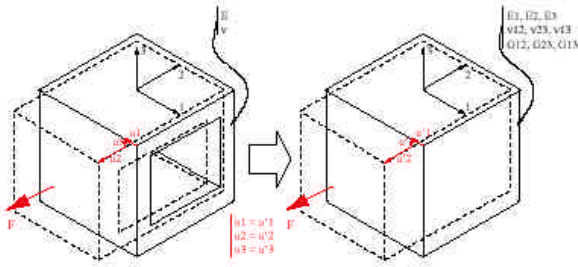


Figure 3 : Model used for evaluate the CP orthotropic equivalent properties

Table 4 : Orthotropic equivalent mechanical properties for CP (1: radial; 2: toroidal; 3: poloidal)

E_1 (MPa)	128000
E_2 (MPa)	87900
E_3 (MPa)	87900
ν_{12}	0.3
ν_{23}	0.137
ν_{13}	0.3
G_{12} (MPa)	49200
G_{23} (MPa)	38700
G_{13} (MPa)	49200

ANALYSES AND RESULTS

In all studied cases, the maximum value of the Von Mises stress in the FW is the consequence of local bending of the channels walls. This value never exceeds about 200 MPa, showing the good withstanding of the FW according to the criteria. In particular, the disconnection of one CP of two (case RT05) – representative of a design necessity to allow PbLi passing from one stage to the stage below [1] - is acceptable.

The SW shows the same kind of local bending as the FW, and the stress level is comparable, thus acceptable. The round corner of the module joining the FW and the SW, leads in general to the same stress level. In some cases, mainly when the CP is disconnected from the BP, a stress peak appears in the BP to SW junction, actually modelled with a sharp (90°) corner. It can be assumed that an appropriate shape can be found in order to reduce this peak under allowable limits. A precise local stress analysis of the CP could not be done because of their simplified modelling. However, the tensile stress in the radial direction (channel direction), in the worst case, i.e. without VP stiffening, has been calculated (RT01, RT02) and is around 150 MPa, which is in the range of acceptable values. A refined local calculation has to be performed to ensure that the criteria are met in the whole CP.

As for the CPs, the VPs have not been precisely modelled. An equivalent thickness has been assumed that respects the real cross section perpendicular to the internal channels.

As the VP are mainly loaded in the channel direction (consequence of the pressure on the cap), the equivalent Von Mises stresses in the VP are therefore relevant, and are nearly equivalent to the primary membrane stresses.

Performed analyses showed that the stress level in the VPs is not acceptable for a pitch over 200 mm (this value does not depend on the cap thickness).

As far as the cups and the BP are concerned, on the basis of the chosen thicknesses, the stress level reached in the models is acceptable.

However, it has to be outlined that stress values are only a rough estimation, since these regions are modelled as simple thick plates.

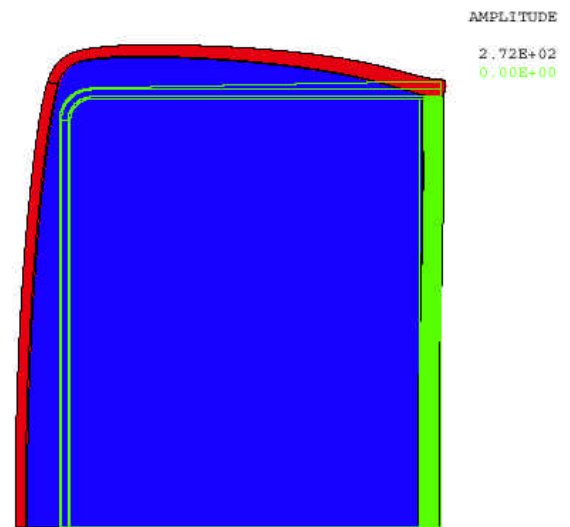


Figure 4 : RT02 model, deformation

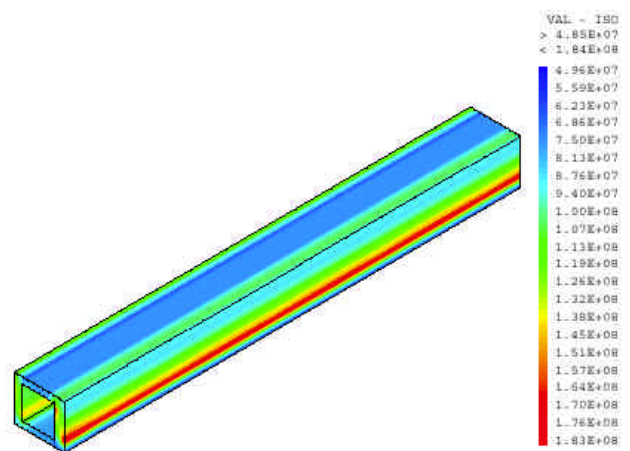


Figure 5 : RT02 model, Von Mises equivalent stresses, FW

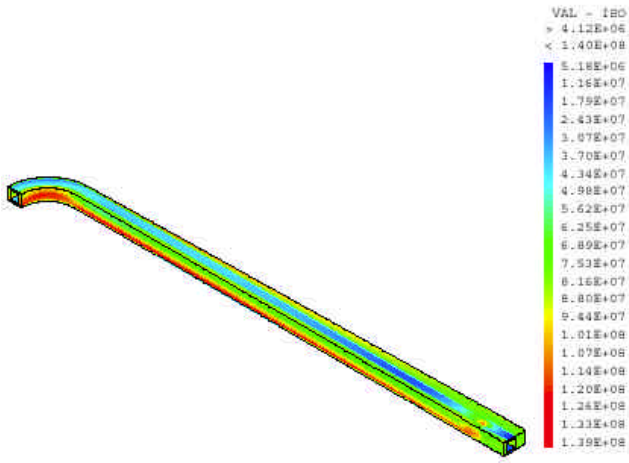


Figure 6 : RT02 model, Von Mises equivalent stresses, SW

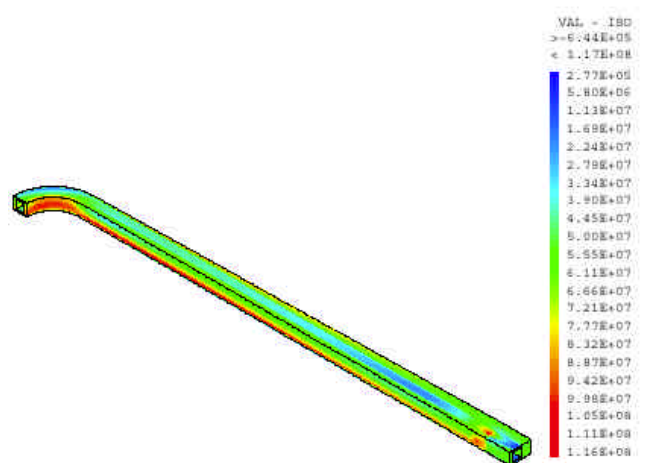


Figure 9 : RT03 model, Von Mises equivalent stresses, SW

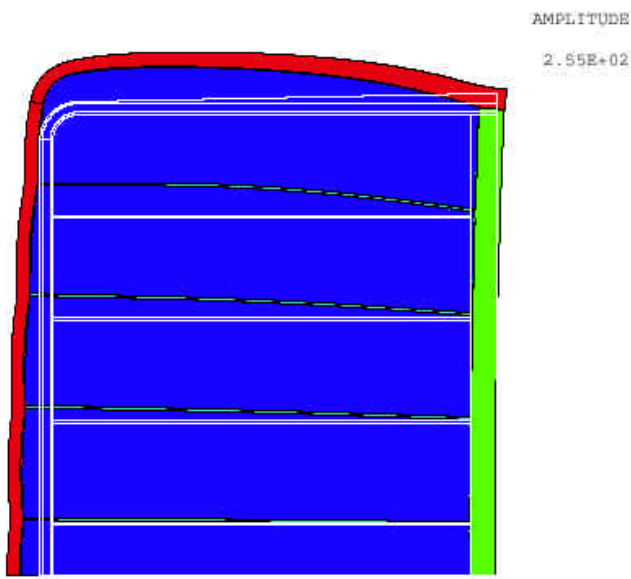


Figure 7 : RT03 model, deformation

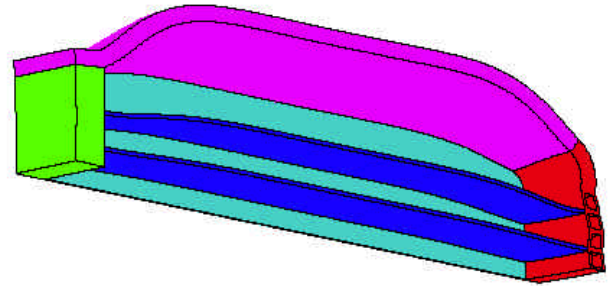


Figure 10 : RP01 model, deformation

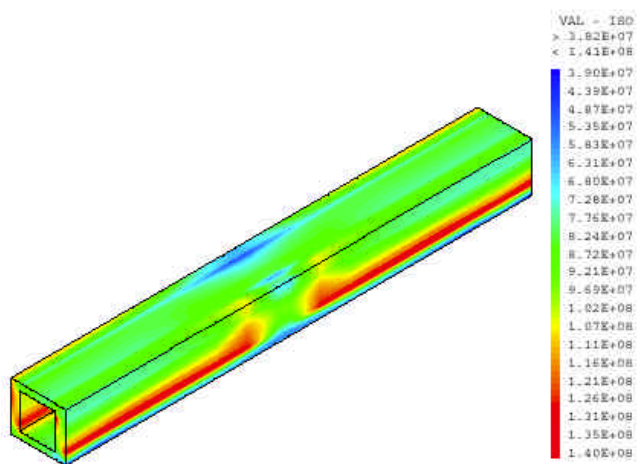


Figure 8 : RT03 model, Von Mises equivalent stresses, FW

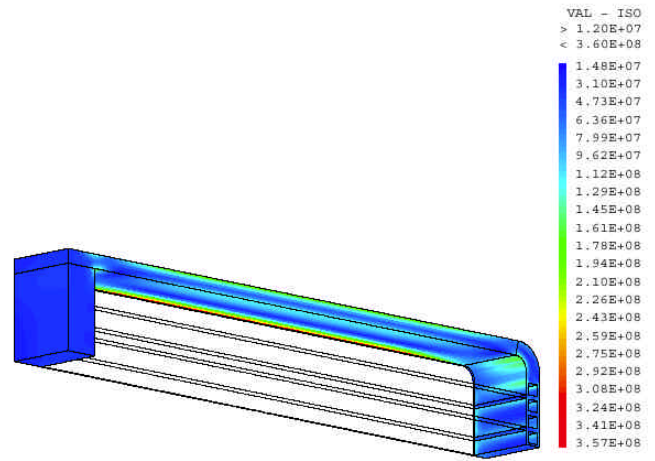


Figure 11 : RP01 model, Von Mises equivalent stresses

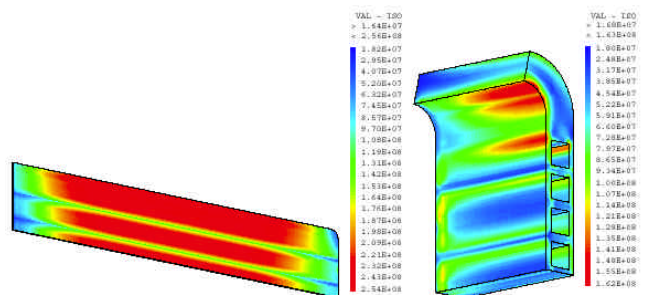


Figure 12 : RP01 model, Von Mises equivalent stresses,
FW and VCP

CONCLUSION

At this step of the design of the HCLL breeding blanket, where only the main dimensions are defined, the accidental internal pressurization of 8 MPa has been simulated and analysed for several geometrical parameters to allow a first optimisation of the needed amount of steel. The results show a good withstanding of the SW and FW, even if CP are disconnected from FW or BP (to allow flowing of the lithium lead). But a vertical stiffening is needed to ensure the cap resistance. The optimised pitch of this stiffening has been defined according to the stiffeners cross section (typically, for an equivalent thickness of the VP of 6 mm, the pitch can not overreach 200 mm).

REFERENCES

- [1] Y. Poitevin et al., "Design conceptual studies for a Helium-Cooled Lithium-Lead Breeding Blanket", CEA report SERMA/RT/02-3191/A, 2002.
- [2] F. Touboul, IISDC (ITER Interim Structural Design Criteria) final report (contract NRT 93-315):part I, CEA report DMT/95/243, 10/05/95.
- [3] F. Tavassoli, "DEMO Interim Structural Design Criteria, DISDC, Appendix A Material design limit data, A.GEN: General, Interim SM 5.1" Report, CEA/CEREM/DECM, September 1999.

REPORTS

G. Rampal et al., "HCLL blanket module design preliminary calculations for accidental pressurization", CEA report SEMT/BCCR/RT/02-055/A, February 2003.

TASK LEADER

Antonella LI PUMA

DEN/DM2S/SERMA
CEA Saclay
91191 Gif-sur-Yvette Cedex

Tél. : 33 1 69 08 79 76
Fax : 33 1 69 08 99 35

E-mail : alipuma@cea.fr

Task Title: COMPLETION OF DESIGN ACTIVITIES ON WCLL AND FINAL REPORT

INTRODUCTION

The Water-Cooled Lithium-Lead (WCLL) Blanket is one of the two European Breeding Blanket lines selected by EU in 1995 [1] with the aim of developing a Fusion DEMO reactor blanket offering suitable tritium breeding, power extraction, neutron shielding, safety and reliability.

Over the years since that time, emphasis has been put on detailed design and R&D of the WCLL Test Blanket Module (TBM) for ITER [2, 3, 4]. The level of design and R&D reached in 2002 [5] constitutes a strong and coherent basis for the insertion of a TBM in ITER since its first day of operation.

However, in 2002, under the constraint of reduction of financial commitments, EU has endorsed the decision [6] to concentrate the work on blanket modules for testing in ITER on a single coolant, Helium. Up to that time, two different coolants were envisaged for the EU Breeding Blankets: i) pressurized water for the WCLL concept and ii) pressurized He for the HCPB concept (Helium-Cooled Pebble-Bed). In order to maintain open the possibility of adopting both types of breeder – lithium-lead and ceramic – the choice of high pressure He coolant has been made, water appearing indeed incompatible with the solid breeder solution (accidental Be/water interaction). Another argument was given for the choice of He: the advantage of higher potential thermodynamic efficiency (expected outlet He temperature: 500°C instead of 325°C for pressurized water at 15.5 MPa).

This, of course, shall be also precisely investigated with regard to design and material (Eurofer) limits under high thermal and neutron loading in a future fusion power plant.

On the other hand, pressurized water technologies requires a lower technological extrapolation from present day state-of-the-art. This offers an advantage within the long term blanket development strategy that should not be definitively precluded.

In that sense, EU indicated [7] that WCLL blanket could be reconsidered in the EU strategy if major problems might be encountered in the development of Helium-cooled PbLi and ceramic concepts.

It appeared then important to close the WCLL activities with a clear list of the reference documents that constitute the status of development of the WCLL concept (in particular of the TBM) and to analyze the major R&D steps that still have to be achieved for the insertion of a WCLL TBM in ITER.

2002 ACTIVITIES

The 2002 activity was aimed at answering to this double objective. The list and main scope of reference WCLL documents can be found in the task report. Hereafter are summarized the major R&D steps that remain to fully qualify a WCLL TBM in ITER

BLANKET MANUFACTURING TECHNOLOGIES

Double-wall-tubes (DWT)

In order to reduce the probability of water leakage in the PbLi, DWT are used for the heat extraction. A ductile interlayer (Cu) is foreseen between two concentric steel tubes with the double objective of i) preventing a potential crack propagation from one tube to the other and ii) maintain a good thermal contact to ensure suitable power extraction. The related technology and its qualification have reached a promising level (quality of joint, dimensional accuracy, bending) [5], but they shall be completed in the future with the following points:

- Reproducibility of satisfactory results obtained on DWT fabrication (with removal of initial gap between tubes before HIP) and DWT bending after HIP. Dimensional accuracy and characterization of joint.
- Bending of more complex 3D shapes (multiple 2D bending in several directions). Dimensional accuracy.
- Confirmation of preliminary results obtained on tube conical expansion at its edges for stiff connection to backplate.
- Development of a double weld scheme for DWT attachment to the back-plate.
- Thermal cycling and endurance tests under relevant WCLL conditions of a C-shape DWT (scale 1:1). Verification of local and global thermal behaviour.
- Thermal cycling and endurance tests under relevant WCLL conditions of a DWT sample (few tens cm) under irradiation. Verification of local thermal behaviour PIE.
- Stress corrosion cracking tests under irradiation. (no PbLi needed).
- Fabrication of a relevant DWT bundle with fixing grid (to be used for tests in a Large-scale Mock-up).

First Wall (FW)

Last R&D results [5] tend to show that the use of mixed solid/powder HIP process for FW fabrication would be the preferred option to avoid damaging of the Cu interlayer around internal cooling tubes. They shall be further completed with the following points.

- Reproducibility of mixed powder/solid HIP FW fabrication. Dimensional accuracy. Optimization of the HIP cycle (temperature, pressure) to avoid local Cu deformation by steel grains. Optimization of grooves design for tube positioning before HIP.
- Fabrication of straight and bent FW.
- Thermal cycling and endurance tests of FW under surface heat flux (same conditions as tests of ITER components).

Segment box (SB)

For the Segment Box, the following activities shall be carried-out:

- Fabrication, with the help of Industry, of a medium-scale demonstrator integrating all selected fabrication and assembly techniques (available industrial technologies), following the reference manufacturing sequence. Verification of the feasibility, optimization and impact of residual stress on global structure. Compatibility of the design and fabrication sequence with the 1% variation in volume due to the martensitic transformation.
- Development of Non Destructive Examination (NDE). Compatibility with fabrication sequence.
- Fabrication of a Large-scale Mock-up (LSMU) produced on the basis of the previous point and integrating instrumentation and electrical heating for testing with Pb-17Li, pressurized water cooling and surface heat flux.
- Testing of the LSMU under relevant conditions (electrical heating simulating neutron power deposition): thermohydraulics, thermal stress, cycling tests.

COATING QUALIFICATION

Al-based coating on outer side of DWT and inner side of SB are envisaged to limit tritium permeation to coolant. Although last studies have shown [5] that low performances of Tritium Permeation Barriers (TPB) would not lead to prohibitive safety effects or incremental capital/operational costs of the WDS (Water Detritiation System), it is necessary to maintain R&D on TPB because: i) safety studies need some confirmation, ii) TPB may remain a cost reduction factor that shall not be precluded, iii) potential benefits of a coating to minimize corrosion and activated corrosion product transport. Two Al-based coating techniques can be envisaged for the WCLL: the CVD (Chemical Vapor Deposition) and the HD (Hot Dipping).

The followings R&D activities should be further carried-out for allowing the use of TPB technology in TBM.

- Definition of a suitable coating procedure for Eurofer substrate (especially surface state preparation before coating). Reproducibility of CVD and HD coating performances in gas and PbLi phases. Evaluation of self-healing.
- Tritium Permeation Reduction Factor (PRF) measurement on Eurofer tube samples (single, DWT) under irradiation.
- Applicability of the CVD and HD process to more complex shapes (plates, corners, etc.). Micrography characterization of coating (uniformity).
- Selection, with the help of Industry, of the most suitable reference coating technique compatible with the reference manufacturing procedure.
- Coating of the LSMU for H/D control testing out-of-tokamak.

PROCESSES AND COMPONENTS

- Instrumentation development: D/T concentration measurement in H₂O Development of a D/T concentration measurement to be used in a Multipurpose Testing Facility (MTF) for T-process testing. If necessary, R&D with limited extrapolation to current technology shall be developed for D concentration measurement in the Multipurpose Testing Facility and, in parallel, T concentration measurement systems in water will be explored in view of TBM testing in ITER.
- Design and fabrication of a MTF for testing of LSMU (thermal-hydraulics, cycling, thermomechanics, permeation, instrumentation) and TBM prior to insertion in ITER.
- LSMU testing in the Multipurpose testing facility.

SAFETY AND LICENSING

One of the main safety issues of the WCLL concept is the interaction between water and PbLi. Both experimental and numerical modeling R&D activities on this subject were launched in parallel in the past years [5]. Significant experimental results have been obtained in 2001-02 with the continuation of the LIFUS-5 campaign (injection of pressurized water in PbLi).

On the other hand, numerical modeling of the thermal interaction using the SIMMER-III code made some significant progress, first, with the preliminary validation of the code on the simplified geometry BLAST experiment and, second with first models of the more complex geometry experiment LIFUS-5. In particular, 2D equivalent model has been developed and shall be further validated and compared to last LIFUS experimental results.

In future years, the following R&D activities should be carried out to validate:

- Effect of large water leak in PbLi. Additional experimental campaign on LIFUS-5 (if required) on the basis of operating parameters defined in collaboration with modelling.
- Development of modelling. Definition of LIFUS experimental parameters. Interpretation of the performed LIFUS experiments. Development and qualification of the geometry modelling and meshing, qualification of physical models including range of relevancy, limitation and sensitivity study. In case a 2D approach would be too limited, 3D capabilities should be implemented in the SIMMER-III code.
- TBM and TBM system safety. Definition of sensors to be used, location in TBM and loops, definition of trip set-points for emergency stop.
- Preliminary Safety Assessment Report.

In addition to this list, detailed R&D priorities that would be required for first 3 years of a re-launched workprogramme on WCLL TBM are given in the activity report.

CONCLUSION

The WCLL Breeding Blanket development activities have been completed and closed with a review of reference documents and analysis of remaining R&D issues up to full qualification of WCLL TBM in ITER. This review shall be used as an entrance point in case of a potential re-launching of WCLL TBM design and R&D activities.

REFERENCES

- [1] L. Giancarli et al., « Water-Cooled Pb-17Li DEMO Blanket line », CEA/Saclay report SERMA/LCA/1801 (1995).
- [2] M. Fütterer et al., « Design Description Document for the European Water-Cooled Pb-17Li Test Blanket Module », in ITER Final Design Report, DDD 5.6.C (1997).
- [3] Y. Poitevin et al., « Status of the design and testing programme of the WCLL Test Blanket Module for ITER-FEAT », CEA/Saclay report SERMA/RT/01-3019/A (2001).
- [4] Y. Poitevin et al., « Fabrication sequence of the WCLL Test Blanket Module for ITER-FEAT », CEA/Saclay report SERMA/RT/01-3020/A (2001).

- [5] Y. Poitevin et al., « WCLL blanket concept: synthesis of last R&D results and impact on the TBM design », CEA/Saclay report SERMA/RT/02-3061/A (2002).
- [6] EFDA Preparatory document for the STAC 2002, EFDA-STAC-T(02)-1/3.2 (2002).
- [7] M. Gasparotto., « Contribution for the preparation of Accompanying Programme in Technology », internal EFDA document, December 2002.

REPORTS

Y. Poitevin et al., "Experience and future R&D needs for a Water-Cooled Lithium-Lead Test Blanket Module", CEA technical report SERMA/RT/02-3190, December 2002.

TASK LEADER

Yves POITEVIN

DEN/DM2S/SERMA
CEA Saclay
91191 Gif-sur-Yvette Cedex

Tél. : 33 1 69 08 31 86
Fax : 33 1 69 08 99 35

E-mail : ypoitevin@cea.fr

Not available on line

Not available on line

Not available on line

Not available on line

Not available on line

Not available on line

Not available on line

Not available on line

Not available on line

Not available on line

Not available on line

Not available on line

Task Title: SAFETY AND LICENSING: Pb-17Li/WATER INTERACTIONS

INTRODUCTION

The general objective of this action is to validate the code models in order to be able to perform safety analyses for licensing.

In that frame, safety studies are specifically devoted to the transient behaviour of a liquid metal breeder blanket module under accidental conditions.

The accident scenario considers the complete failure of a water tube (coolant) into the lithium/lead (Li/Pb) blanket which was previously investigated through the experimental BLAST tests and which is under analysing through the new and more detailed experimental LIFUS programme at Brasimone.

During the first part of the accident scenario the violent thermal interaction between “hot” Li/Pb and injected “cold” water leads to a pressure transient, due to a rapid water vaporization, which is analysed using the Simmer-III code (multi-phase and multi-component thermohydraulics in a 2D geometry).

In a first study, code physical models and code options are widely investigated upon the BLAST experiments numerical simulation in order to select the most appropriate code parameters to correctly reproduce the involved key phenomena ; in a second study, the selected code parameters are applied to the LIFUS 5 test numerical simulation.

The general experimental device provides for:

- a cylindrical reaction vessel containing or not tube bundles and filled with liquid Li/Pb,
- a pressurised water injector into the reaction tank at the bottom of the vessel,
- an expansion tube joining the top of the reaction vessel to a cylindrical expansion tank partially filled with liquid Li/Pb.

The main experimental parameters concern the water injection conditions (temperature and pressure), the Li/Pb temperature and the presence of obstacles inside the reaction vessel, the expansion tube diameter.

The pressure evolution in the reaction tank is recorded during the test.

2002 ACTIVITIES

A scheme of the LIFUS 5 experiment is shown in figure 1.

The main elements of the LIFUS experiment, modeled with SIMMER-III are:

- the interaction tank (S1) ;
- the expansion tubes ;
- the expansion tank (S5).

The additional components of the experiment, which are not represented, are:

- the liquid water tank and the feeding pipe (S2) ; they are modeled using a boundary condition ; the problem is treated assuming an instantaneous contact between water and lithium/lead ; this will be improved in a later approach,
- the safety tank (S3) connected to the expansion tank which allows to collect the gaseous and aerosol products at the end of the test.

The experiment is represented in Cartesian coordinates in order to better represent dissymmetrical phenomena such as turbulence.

In view of the complexity of the 3D geometry of the experiment, the main difficulties were, on the one hand, to find a representative section view of the interaction tank, and on the other hand, to take into account the effect of the 3rd dimension, so as to correctly represent the tank/expansion tube junctions.

The proposed representation models:

- the 3D position of the ‘U’ tubes versus the injector ;
- the four interaction tank compartments separated by walls ;
- the free space between the walls and the lateral wall of the interaction tank ;
- the expansion tubes associated to each of the four compartments ;
- the free volume of the expansion tank.

The injection conditions (liquid water, pressure, temperature) are imposed on the upper boundary of the first mesh of the injector.

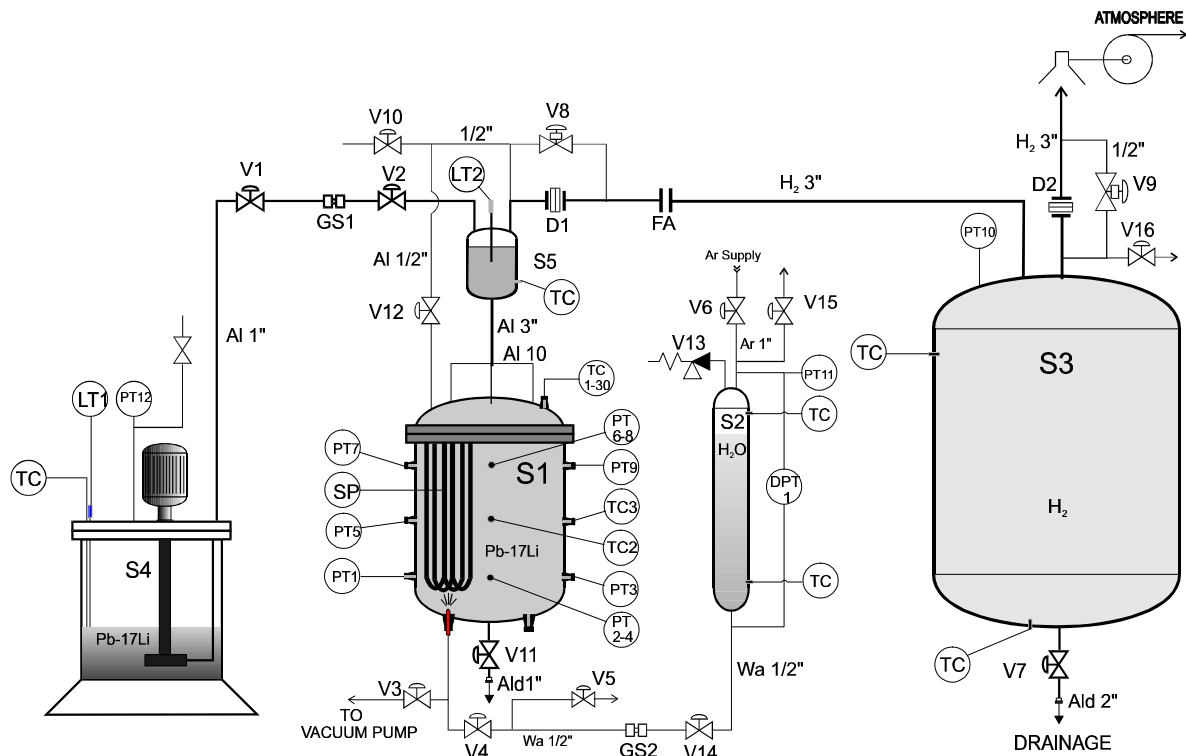


FIG. 1

Figure 1 : LFUS 5 facility

For test n°4 the initial conditions are the following:

- LiPb temperature: 330°C,
- temperature/pressure of injected water: 325°C/ 15.5 Mpa,
- length of the injector: 120 mm.

The meshing is defined mainly in the interaction tank by square meshes so as to not favor one of the two directions during the formation and evolution of the jet. The discretization chosen is sufficiently fine for the experimental dimensions of the tanks and tubes.

Fine meshing around the specificities of the domain (injector/interaction tank, tank/expansion tube connection) was not possible as it would have affected the numerical current condition and significantly increased the calculation time.

A design basis factor is calculated so as to ensure a good agreement between the experiment geometry and that modeled in the Cartesian representation. This factor is deduced from the proportionality between the value of the main compartment of the modeling, adjusted to that of the experiment (25 liters).

This choice indirectly supposes that during the thermal interaction phase between water and lithium/lead, the steam bubble mostly stays confined in the main interaction tank compartment until the system is pressurized.

This is confirmed by the calculations as shown on the figure 2.

In the Cartesian representation, this factor mainly affects the hydraulic characteristics of the tubes (hydraulic diameter, flow through section, friction surface), as well as the free volume of the expansion tank. Singular pressure drop coefficients were introduced in the calculation. In the modeling, this concerns the injector, the obstacle tube bundle, the porous wall and the expansion tubes.

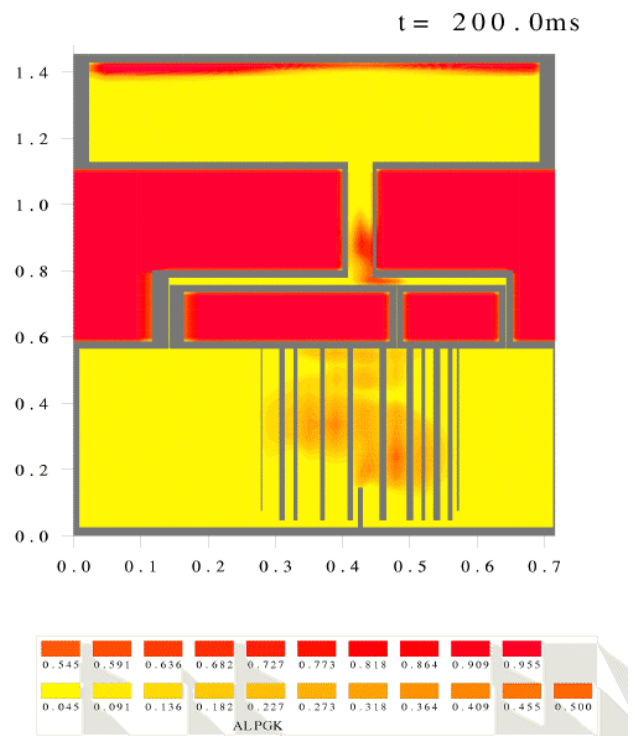


Figure 2 : SIMMER-III calculation, LIFUS-5 test n°4, steam repartition at 200 ms

CONCLUSIONS

This calculation shows that:

- the water injected in the interaction tank nearly instantaneously vaporizes until the end of the transient (1000 ms) ;
- the general behaviour of pressure waves in the interaction and expansion tanks is comparable to that of the test ; when the pressure level in the expansion tank becomes significant, an increase in pressure is seen in the interaction tank ;
- the delay needed to pressurize the system is of the same order of magnitude as that of the test ;
- the hypothesis of changing to a Cartesian representation is verified ; the steam bubbles mostly stays confined in the main compartment of the interaction tank.

REPORTS AND PUBLICATIONS

P. Sardain, T. Jeanne, "Cartesian representation of LIFUS 5 with the SIMMER III code and application to the test n° 4", CEA report DER/SERI/LFEA 02/5019.

TASK LEADER

Pierre SARDAIN

DER/SERI/LFEA
CEA Cadarache
13108 Saint Paul Lez Durance Cedex

Tél. : 33 4 42 25 37 59

Fax : 33 4 42 25 36 35

E-mail : pierre.sardain@cea.fr

Not available on line

Not available on line

Not available on line

Not available on line

Not available on line

Not available on line

Task Title: DEVELOPMENT OF CERAMIC BREEDER PEBBLE BEDS

Characterization of Li_2TiO_3 pebbles

INTRODUCTION

The characterization of Li_2TiO_3 pebbles, in support of both their fabrication technology and the investigation of the performance of Li_2TiO_3 pebbles and pebble beds, plays a major role in the development of Li_2TiO_3 pebbles for the HCPB blanket.

The work in 2002 addresses essentially two items:

- Detailed characterization of the Li_2TiO_3 pebbles of the 6 kg-batch produced in 2001.
- Pre-test and post test examinations of Li_2TiO_3 pebbles.

2002 ACTIVITIES

Focus in 2002 was placed on the determination of:

CHARACTERISTICS OF THE Li_2TiO_3 PEBBLES OF THE 6 kg BATCH PRODUCED IN 2001 AT CERAMIQUES TECHNIQUES ET INDUSTRIELLES

It is recalled that one of the deliverables of the 2001 program activity was the production by pre-industrial means of a 6 kg-batch of Li_2TiO_3 pebbles at the end of the year. The goal of this production was a dual one:

- produce an amount of Li_2TiO_3 pebbles sufficient to control the fabrication process parameters,
- produce an amount of Li_2TiO_3 pebbles necessary and sufficient to supply the campaign of the functional tests of Li_2TiO_3 pebble beds foreseen in 2002. Among others, 3 kg of Li_2TiO_3 pebbles were delivered in February for the HE-FUS 3 mock-up tests at ENEA.

Thus, a batch of 6 kg of 1 mm Li_2TiO_3 pebbles, reference "CTI 9A1 Ti 1100 CTI" comprising 6 sub-batches has been produced in December 2001, following the procedure described in [1]. This batch of Li_2TiO_3 pebbles was sintered at 1100°C. Relevant characteristics, i.e., pebble bed density, pebble open/closed porosity, grain size, specific surface area, and average crush load of the sub-batches have been determined.

One can observe that the uniformity of the sub-batches is relatively satisfactory showing that temperature conditions throughout the industrial furnace are quite uniform. However, the density of the sub-batches is lower than the goal value (~ 90 % of theoretical density).

A cross section of Li_2TiO_3 pebbles observed by optical microscopy shows that there are large holes in the pebbles.

Investigations at CTI have shown that there has been a problem with the extrusion apparatus during the fabrication of this batch.

The level of vacuum in the extrusion chamber was poor and air bubbles were introduced in the paste resulting for the pebbles in a low density. After repair of the extrusion apparatus, a new batch of Li_2TiO_3 pebbles, reference "CTI 1532 Ti 1100 CEA" has been produced in March.

The density of pebbles, around 89 % of theoretical density, is in agreement with the objective.

PRE-TEST AND POST-TEST EXAMINATIONS OF Li_2TiO_3 PEBBLES

In order to evaluate the performance of the Li_2TiO_3 pebbles and, as a consequence, to improve it, if needed, relevant functional tests of pebble beds both out-of-pile and in-pile are carried out in collaboration with FZK and NRG.

Checking the characteristics of the Li_2TiO_3 pebbles before and after the out-of-pile tests is carried out at CEA in order to identify any changes and, thereby, help interpretation of test results.

Characteristics of Li_2TiO_3 pebbles for the HICU experiment

Among the criteria for the selection of the ceramic breeder for the HCPB blanket is the behaviour of the pebble beds under EOL lithium burn-up and dpa conditions. The behaviour of the two ceramic breeder options (Li_4SiO_4 and Li_2TiO_3) will be studied in the HICU experiment to be started in 2003 in HFR.

For the Li_2TiO_3 pebbles specimens, three ^6Li enrichments are necessary to cover the objectives of the experiment. Adjustments of the process were necessary because of the slightly different characteristics of the ^6Li -enriched lithium precursors. Characteristics of the specimens are given in table 1.

In addition, three samples were prepared for the HICU experiment: a) smaller pebbles developed in 2002, b) same pebbles as in the submodule experiment (started in 2002), and c) pebbles representative of industrial fabrication.

These three samples have a natural ^6Li enrichment. Characteristics of the samples are also given in Table 1. These six samples were delivered in June to NRG for the HICU experiment.

*Table 1 : Characteristics Li_2TiO_3 pebbles
for HICU experiment*

Reference	Pebble size (mm)	Porosity (%)		Bed density (g/cm^3)	Grain size (μm)	Average crush load (N)	Remarks
		Open	Closed				
CTI 1890 Ti 1100 CEA	0.8 - 1.2	12.5	4.4	1.68	1 - 3	34	0.06 % ^6Li -enrichment
CTI 2090 Ti 1140 CEA	0.8 - 1.2	13.2	5.1	1.68	1.5 - 4	41	11 % ^6Li -enrichment
CTI 2590 Ti 1100 CEA	0.8 - 1.2	7.5	5.9	1.73	1 - 3	51	29.5 % ^6Li -enrichment
CTI 942 Ti 1100 CEA	0.6 - 0.8	2.0	4.9	1.91	1 - 4	31	Smaller pebbles and natural enrichment
CTI 1271 Ti 1100 CEA	0.8 - 1.2	4.2	5.5	1.85	1.5 - 5	40	In submodule experiment and natural enrichment
CTI 1532 Ti 1100 CEA	0.8 - 1.2	6.0	5.3	1.82	1.5 - 5	31	Industrial fabrication and natural enrichment

In 2002, tests were carried out at CEA on the Li_2TiO_3 pebbles:

Annealing test at 970°C in air at CEA during three months

One important issue for the HCPB blanket is the maximum temperature allowable for the ceramic breeder. Among phenomena, which can limit the upper operating temperature, are phase changes occurring with large density changes, lithium vaporization, and change of microstructure (grain growth) on annealing. For sintered Li_2TiO_3 pebbles, the third phenomenon is likely to be the limiting one. It is investigated with annealing tests.

This test was made at CEA within the framework of the pebbles optimisation. It aimed at comparing the behaviour of the Li_2TiO_3 pebbles as a function of their sintering temperature, in other words, as a function of their microstructure. The temperature and time conditions of this test (970°C, 3 months) are representative of DEMO end-of-life conditions at the higher temperature of the breeder in the HCPB blanket. In view of the results obtained with the Li_2TiO_3 pebbles sintered at 1050°C in 2001, this new annealing test at 970°C with the pebbles sintered at 1100°C was decided.

Characteristics of the specimens (weight loss, open and closed porosity, crush load, and grain size) were checked on the initial pebbles and on pebbles annealed in air at 970°C during 1 month, 2 months, and 3 months, respectively. After the annealing test, a significant reduction of the closed porosity was observed. The average crush load decreases slightly from 34 N to 28 N. During the aging there was an increase in the grain size. After 3 months, it grew up to about 18 μm . X-ray diffraction analysis on the annealed pebbles shows only the monoclinic Li_2TiO_3 phase.

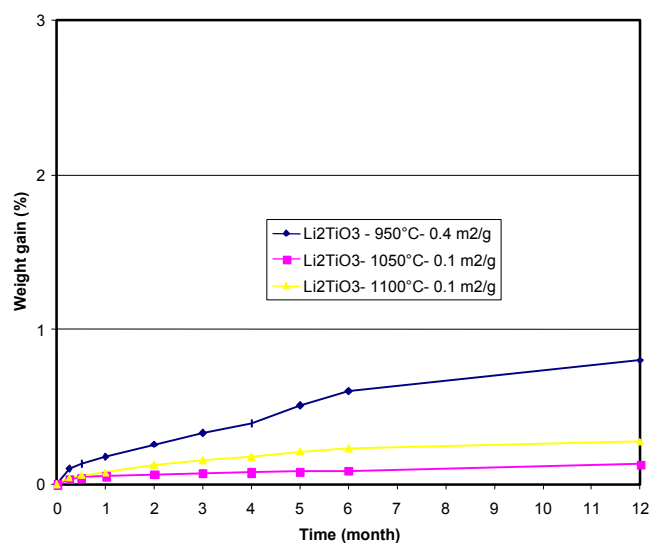


Figure 1 : Weight gain of Li_2TiO_3 pebbles on air exposure

In conclusion of these different tests, grain growth observed for the Li_2TiO_3 pebbles sintered at 1100°C is very similar to that for the Li_2TiO_3 pebbles sintered at 1050°C, but is less important than for the Li_2TiO_3 pebbles sintered at 950°C.

Sensitivity to moisture of Li_2TiO_3 pebbles in air during twelve months

Lithium ceramics are hygroscopic materials. It was previously shown that hygroscopy increases with the $\text{Li}_2\text{O}/\text{MO}$ ratio in the composition ($\text{M}=\text{Al}, \text{Zr}, \text{Ti}, \text{Si}$) [2]. Further, hygroscopy increases with increasing specific surface area of the material. Previous studies also showed that moisture adsorption and subsequent CO_2 reaction have a deleterious effect on ceramic breeder materials relevant properties.

Precautions against moisture may therefore be necessary during materials fabrication, storage, and loading of the ceramics in the reactor, which makes these operations very heavy.

Moisture sensitivity of Li_2TiO_3 pebbles has been studied at CEA by measuring at room temperature the weight gain of pebbles as a function of time on air exposure (relative humidity in the 40 %-60 % range). Figure 1 shows weight gain as a function of time for Li_2TiO_3 pebbles with different specific surface areas. A weight gain of less than 1 % after one year is measured for Li_2TiO_3 pebbles with the higher specific surface area and of 0.2 % for the reference pebbles. It can be concluded that Li_2TiO_3 pebbles do not practically react with air at room temperature.

The unsensitivity of Li_2TiO_3 pebbles to moisture seems to be a specific feature of the Li_2TiO_3 ceramic. This is a significant advantage with respect to fabrication and storage of industrial scale as well as with respect to blanket loading in the reactor.

CONCLUSION

The CEA activity regarding the characterization of the Li_2TiO_3 pebbles was achieved in accordance with the foreseen time schedule. Specimens for the functional tests of pebble beds, and for the irradiation experiments were delivered in due time to the European partners. In addition, comparing the characteristics of the Li_2TiO_3 pebbles before and after the out-of-pile tests of pebble beds, performed so as to evaluate the performance of the Li_2TiO_3 pebbles option, was very useful to help understanding any phenomena occurring during the tests.

REFERENCES

- [1] J.D. Lulewicz, N. Roux, F. Pourchet, J.P. Joulin. Status of fabrication of Li_2TiO_3 pebbles by extrusion-spheronisation-sintering process. Presented at CBBI-10, Karlsruhe (Germany), October 2001.
- [2] B. Rasneur. Storage of porous lithium ceramics. Internal report CEA/CEREM/CE2M/LECMA 94/016, December 1994.

REPORT AND PUBLICATIONS 2002

J.D. Lulewicz. Interim report of the activity from January 2002 through June 2002 on sub-tasks TW2-TTBB-005a-D3 and TW2-TTBB-005a-D4. Internal report CEA/SE2M/LECNAM 02-DT-007. June 2002.

J.D. Lulewicz. Final report on sub-tasks TW2-TTBB-005a-D3 and TW2-TTBB-005a-D4. Internal report CEA/SE2M/LECNAM 02-RT-014. December 2002.

TASK LEADER

Jean-Daniel LULEWICZ

DRT/LIST/DECS/SE2M/LECNAM
CEA Saclay
91191 Gif-sur-Yvette Cedex

Tél. : 33 1 69 08 48 24
Fax : 33 1 69 08 57 54

E-mail : jean-daniel.lulewicz@cea.fr

Task Title: DEVELOPMENT OF CERAMIC BREEDER PEBBLE BEDS

Mastering and optimising of process parameters for the preparation of Li_2TiO_3 powder and for the fabrication of Li_2TiO_3 pebbles

INTRODUCTION

Li_2TiO_3 pebbles are developed at CEA as candidate ceramic breeder option for the Helium-Cooled-Pebble-Bed (HCPB) blanket investigated in Europe. The extrusion-spheronisation-sintering process was selected in 1996 in order to produce Li_2TiO_3 pebbles fulfilling the HCPB blanket requirements, and was developed with the collaboration of the industrial firm Céramiques Techniques et Industrielles.

From 1996 to 2001, the investigation was mainly focused on:

- The optimisation of the Li_2TiO_3 pebbles and their characterisation with the study of the fabrication process parameters which control the characteristics (shape, size, density, specific surface area, grain size, strength, crystal phases and purity level) of the pebbles. Indeed, these characteristics govern the performance of the Li_2TiO_3 pebbles and of the Li_2TiO_3 pebble beds.
- The finalisation of the fabrication facility.

The work in 2002 addresses essentially four items:

- Investigation of the lower limit of pebble diameter using the extrusion process.
- Enhancement of production yield of Li_2TiO_3 .
- Investigation with ENEA of the feasibility of lithium recycling.
- Production of a 6 kg-batch of Li_2TiO_3 pebbles with the improved 2002 process.

2002 ACTIVITIES

INVESTIGATION OF THE LOWER LIMIT OF PEBBLE DIAMETER USING THE EXTRUSION PROCESS

The current sintered Li_2TiO_3 pebbles have diameters in the range 0.8 mm to 1.2 mm. Investigation was started in 2001 [1] to determine the lower limit of Li_2TiO_3 pebble diameter achievable with the extrusion process with a view to find out any benefit of smaller pebbles for the design of the Helium-Cooled-Pebble-Bed blanket. Indeed, smaller pebbles can be advantageous to better fill the ceramic breeder space and to increase pebble bed density and thermal conductivity. In 2002, an attempt was made to

obtain a better sphericity of the pebbles and to decrease, if possible, the pebble diameter down to 0.5 mm. A new revision of the formulation of the extrusion paste in order to improve the sphericity was decided. The amount of binder and plasticizer was twice higher than for the current extrusion paste. The fabrication process parameters were once more adjusted in order to obtain Li_2TiO_3 pebbles with a smaller diameter. First, a nozzle of 0.8 mm instead of 1 mm was used during the extrusion step and the cutting system was revised for the cutting step of the smaller granules. However, the same extrusion machine and the same spheronization device as for the preparation of the current pebbles were used for these trials. A batch of 300 g of smaller Li_2TiO_3 pebbles was produced in April 2002. The pebbles of this batch were sintered at 1100°C at CEA and characterized at CEA. The size, the shape and the microstructure of the smaller Li_2TiO_3 pebbles were observed using scanning electron microscopy and optical microscopy. As shown in figure 1, the shape is close to spherical, and the pebble size distribution is 0.6 to 0.8 mm.

The microstructure is homogeneous, and grain size is 1 to 4 μm . A comparison of the characteristics of the 0.8-1.2 mm Li_2TiO_3 pebbles with the characteristics of the 0.6-0.8 mm Li_2TiO_3 pebbles shows that open porosity decreases significantly and closed porosity decreases slightly for the smaller pebbles. Pebble bed density increases significantly which is advantageous. Grain sizes are very similar for both diameter pebbles sintered at 1100°C.

The feasibility to produce small Li_2TiO_3 pebbles in the range 0.6 mm to 0.8 mm with the extrusion process was shown in this study and pebbles characteristics are very promising. It is expected that this diameter range is the lowest one achievable using the extrusion-spheronisation-sintering process. In any case, going to even smaller pebbles does not seem desirable.



Figure 1 : Shape of smaller Li_2TiO_3 pebbles

ENHANCEMENT OF PRODUCTION YIELD OF Li_2TiO_3

The cutting step is the rate limiting step of the fabrication process in term of capacity for the mass production of Li_2TiO_3 pebbles. A redesign of the cutting device to obtain the cylindrical granules was decided in order to improve the production rate.

The new apparatus is shown in figure 2. A batch of 300 grams of smaller Li_2TiO_3 pebbles was produced in September 2002 in order to validate the process with the new cutting device. The pebbles of this batch were sintered at 1100°C at CEA and characterized at CEA. The characteristics of these pebbles are very similar to the characteristics of the smaller pebbles presented in above section.

The size, the shape and the microstructure of the Li_2TiO_3 pebbles were observed using scanning electron microscopy and optical microscopy. The shape is close to spherical, and the pebble size distribution is 0.6 to 0.8 mm. It will be possible in the future to produce a larger quantity of granules with this new cutting device (set of gear wheels) than with the old system (several knives in parallel) during the same time.



Figure 2 : Old cutting system (on the left) and new cutting device (on the right) to produce the Li_2TiO_3 granules

INVESTIGATION WITH ENEA OF THE FEASIBILITY OF LITHIUM RECYCLING

A wet chemistry process is developed at ENEA [2] for extracting lithium from Li_2TiO_3 in the form of Li_2CO_3 powder. This process will be used for the recovery of ^6Li from a lithium titanate breeder burned up to its end of life in the European HCPB blanket.

The process was optimised at ENEA with respect to the chemical attack of lithium titanate and with respect to the precipitation of carbonate from aqueous solutions to get a Li_2CO_3 powder, with the suitable chemical and morphological characteristics specified by CEA. Next, the Li_2CO_3 powder will be used in the extrusion process of fabrication of Li_2TiO_3 pebbles by CTI.

In order to simulate a real reprocessing of Li_2TiO_3 breeder, the procedures, first set up at ENEA with Li_2TiO_3 powder, have been confirmed by using sintered Li_2TiO_3 pebbles delivered by CEA. A batch of 400 grams of Li_2CO_3 powder was produced by ENEA in 2001. It was used at CEA to fabricate fresh Li_2TiO_3 powder in order to demonstrate the feasibility of ^6Li recycling, a must in the future. The following procedure was used for the preparation of the Li_2TiO_3 powder at CEA.

A mixture of titanium oxide powder freshly passed through a $400\ \mu\text{m}$ screen and lithium carbonate powder freshly passed through a $200\ \mu\text{m}$ screen is prepared to obtain a material with a slight lithium deficiency (5 %). The first reaction takes place at 700°C for 3 hours resulting in a weight loss of around 27 % corresponding to a reaction yield of 90 %. After passing through a $200\ \mu\text{m}$ screen, the powder is once again heated to 800°C for 3 hours to complete the reaction. A weight loss of 3 % is then observed. Comparison of characteristics of the current Li_2TiO_3 powder and of the Li_2TiO_3 powder from reprocessed Li are presented in table 1. Characteristics include X-ray diffraction analysis, weight loss on Li_2TiO_3 formation, powder apparent density, specific surface area, and particle diameter. As can be seen in table 1, all results are close one to the other, which is satisfactory. According to expectations, X-ray diffraction analysis shows monoclinic Li_2TiO_3 as major phase, and traces of $\text{Li}_4\text{Ti}_5\text{O}_{12}$ due to the lithium substoichiometry being aimed at.

Elemental impurities contents were measured by Spark Source Mass Spectrometry. An increase to 430 ppm in Sodium is observed in the Li_2TiO_3 powder from reprocessed Li. The origin of Sodium is due to the process developed at ENEA. In fact, the precipitation of carbonate from the aqueous solution to get a Li_2CO_3 powder is obtained with an excess of sodium carbonate. An attempt is necessary at ENEA to decrease the sodium content in the Li_2CO_3 powder.

Table 1 : Characteristics of Li_2TiO_3 powders

	Current Li_2TiO_3 powder	Li_2TiO_3 powder from reprocessed Li
X-ray diffraction	Monoclinic Li_2TiO_3 + traces of $\text{Li}_4\text{Ti}_5\text{O}_{12}$	Monoclinic Li_2TiO_3 + traces of $\text{Li}_4\text{Ti}_5\text{O}_{12}$
Total weight loss	29.8 %	29.5 %
Specific surface area	$4.0\ \text{m}^2/\text{g}$	$2.9\ \text{m}^2/\text{g}$
Mean particle size	$0.6\ \mu\text{m}$	$0.61\ \mu\text{m}$
Apparent density	$0.38\ \text{kg/l}$	$0.49\ \text{kg/l}$

FABRICATION OF A 6 kg BATCH OF Li_2TiO_3 PEBBLES

In order to master the fabrication process parameters as improved in 2002, as well as to dispose of the amount of Li_2TiO_3 pebbles necessary to supply the campaign of functional tests of Li_2TiO_3 pebble beds and HCPB mock-up tests foreseen in 2003, a 6 kg-batch of Li_2TiO_3 pebbles with the size distribution in the range 0.6 to 0.8 mm was produced at the end of 2002.

CONCLUSION

The activity at CEA regarding mastering and optimisation of the fabrication parameters of the extrusion-spheronization-sintering process for the production of Li_2TiO_3 pebbles was achieved in accordance with the foreseen time schedule.

To summarize the activity at CEA in the last few years, a fabrication process was finalized to produce Li_2TiO_3 pebbles capable to fulfil the design requirements stated by the HCPB blanket design team. The work was mostly guided by the results of the out-of-pile testing of Li_2TiO_3 pebble beds. The lack of tritium release and irradiation behaviour results was detrimental to the completeness of Li_2TiO_3 pebbles optimisation. The development of Li_2TiO_3 pebbles has demonstrated that a wide range of pebbles characteristics can be obtained by the extrusion process, allowing to tailor the properties/performance of the Li_2TiO_3 pebbles/pebble beds according to a variety of design requirements. With the present facility at CTI, a production of 150 kg/year can be obtained, and extrapolation of the production to industrial scale is not expected to raise any significant problem since the extrusion process makes use of conventional, well-proven techniques of ceramic industry.

Based on the present HCPB blanket design requirements, and on the experimental results available to date, specifications for the Li_2TiO_3 powder and Li_2TiO_3 pebbles can be given for industrial scale fabrication. Possible modification of the design requirements could be accommodated owing to the flexibility of the process.

REFERENCES

- [1] J.D. Lulewicz, N. Roux, F. Pourchet, J.P. Joulin. Status of fabrication of Li_2TiO_3 pebbles by extrusion-spheronisation-sintering process. Presented at CBBI-10, Karlsruhe (Germany), October 2001.
- [2] C. Alvani et al. Li_2TiO_3 pebbles reprocessing, recovery of ^6Li as Li_2CO_3 . Presented at CBBI-10, Karlsruhe (Germany), October 2001.

REPORT AND PUBLICATIONS 2002

J.D. Lulewicz. Interim report of the activity from January 2002 through June 2002 on sub-tasks TW2-TTBB-005a-D3 and TW2-TTBB-005a-D4. Internal report CEA/SE2M/LECNAM 02-DT-007. June 2002.

J.D. Lulewicz. Final report on sub-tasks TW2-TTBB-005a-D3 and TW2-TTBB-005a-D4. Internal report CEA/SE2M/LECNAM 02-RT-014. December 2002.

J.D. Lulewicz, N. Roux. Fabrication of Li_2TiO_3 pebbles by the extrusion-spheronisation-sintering process. Journal of Nuclear Materials 307-311 (2002) 803-806.

TASK LEADER

Jean-Daniel LULEWICZ

DRT/LIST/DECS/SE2M/LECNAM
CEA Saclay
91191 Gif-sur-Yvette Cedex

Tél. : 33 1 69 08 48 24

Fax : 33 1 69 08 57 54

E-mail : jean-daniel.lulewicz@cea.fr



The studied HCLL concept is essentially formed by a directly He-cooled steel box having the function of PbLi container and by a series of horizontal cooling plates (CP) for heat extraction in the breeder zone. He is flowing inside those cooling plates in internal U-shape tubes (see later in document).

The box structure is also reinforced by radial vertical He-cooled stiffening plates allowing the box to resist to an accidental 8 MPa internal pressurization. Only one He cooling circuit is foreseen for the module. The He inlets first in the FW at 300°C and flows toroidally in internal channels. It exists then the FW at around 353°C and is then distributed from the back of the module to the breeder zone, flowing inside horizontal and vertical cooling plates.

The He is then collected at the back again and exists at an optimised temperature of 470°C (the maximum acceptable value with regard to design limits, see below). The PbLi breeder is slowly flowing between horizontal cooling plates from the top of the module to the bottom. Some holes have been designed in cooling plates, alternatively in the front and back part to allow PbLi passing from one stage to the stage below.

The He collector system of this concept appeared to be one of the main critical point of the design. Details can be found in the activity report, but it shall be noted here that some points appeared particularly difficult and could necessitate further design improvements or changes (see conclusion).

Table 1 summarizes main geometrical data and operating parameters for this concept after iteration of analyses.

THERMAL AND THERMO-MECHANICAL ASSESSMENT

Thermal hydraulic evaluations have been performed coupled with thermo-mechanical FEM analyses. The CASTEM FE code has been used for these ones.

Model description

The assessment has been carried out on the basis of the reference HCPB geometry [1]. The FW and side walls are cooled by horizontal square channels, the section of which can vary as a function of the heat load. $16 \times 16 \text{ mm}^2$ being the nominal cross section, the dimensions of the channel should assume the value of $16 \times 38 \text{ mm}^2$ in the more solicited section (surface heat flux of 0.5 MWm^{-2} and neutron wall load of 2.4 MWm^{-2}). The cooling of the BZ is ensured by horizontal coolant/stiffening 5 mm thick cooling plates, where are drilled square U-channels of section $3 \times 3 \text{ mm}^2$.

These channels are radially oriented, so the He enters from one leg and it is routed back from the other one in the rear of the module. Previous studies carried out on the I-HCPB concept [2] showed that, due to small pitch between the tubes, some heat transfer takes place from the hot leg to the cold leg of the same channel, so decreasing the efficiency of the cooling.

Table 1 : Main design and operational parameter for the generic HCLL breeder blanket module

Typical module dimensions	Pol 2 m x Tor 4 m x Rad. 1 m
Heat and neutron load	HF = 0.5 MW/m^2 , NWL = 2.4 MW/m^2
First Wall	
He cooling	Toroidal – single direction
Thickness	25 mm (4/16/5 mm)
Cooling channels	(16 x 38) mm^2 Pitch between tubes 22 mm 90 tubes
He flow velocity	78 m/s
Q _{tot}	47.8 kg/s
P _{in} He	80 bars
ΔP He	~ 1 bar (derived from I-HCPB)
T inlet/outlet FW He	300/353 °C
FW He collectors	(320 x 320) mm^2 (for v = 40 m/s)
Fabrication (preferred option)	From square tubes (FW bending easier)
Cooling plates	
Pitch between plates / number	44 mm / 900 (45 pol x 20 tor)
Cooling channels	(3 x 3) mm^2 – pitch 5 mm
thickness	5 mm (1/3/1 mm)
He flow velocity	25 m/s
Q VP	~ 90% Q _{tot}
T inlet/outlet He	353/470 °C
ΔP He	~ 0.1 bar (derived from I-HCPB)
CP collectors	15 x 15 mm^2 (v = 20 m/s)
T max He in CP	500 °C
Fabrication	2-steps HIP process
Vertical plates	
Pitch between plates / number	200 mm / 19
Cooling channels	(3 x 3) mm^2 – pitch 10 mm
thickness	7 mm (2/3/2 mm)
He flow velocity	28 m/s
Q VP	~ 10% Q _{tot}
T inlet/outlet He	353/470 °C
VP collectors	34 x 34 mm^2 (v = 20 m/s)

This effect could be reduced using bundles of more tubes, in particular, I-HCPB studies shown that a suitable solution could be to use bundles of three channels like shown in figure 4.

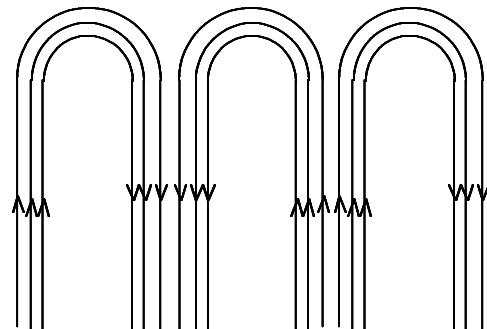


Figure 4 : He circulation scheme in the BZ horizontal cooling plates

Materials and criteria

The Pb-17Li physical properties used for the analyses are taken from [3]. The laws describing the physical properties, validated until to 600°C, have been extended to higher temperatures.

Properties of the 9Cr-1Mo ferritic-martensitic steel as described in [4] have used for steel structures.

Studies on Fe-(8-9)% Cr reduced activation steels showed that good creep resistance exists for temperatures up to ~550°C, but poor creep resistance occurs at 600°C [5], thus the high temperature limits of about 550°C is generally accepted [6].

Thermal-hydraulic and thermal results

In the thermal-hydraulic scheme, the He cools in series the FW and the BZ, where it flows in parallel in the horizontal and vertical plates. Then it is collected towards the steam generator.

Once the power deposited on the module is known and He inlet and outlet temperatures are imposed, the gas mass flow in a module is determined by the enthalpy balance. The He average velocity in the channels is also found by a mass balance, once the cross sections and number of channels are fixed.

Supposing that He flowing in the FW recovers the heat deposited in it (and 10 % of the one deposited on the BZ) the FW outlet temperature, that is also the CPs inlet temperature is fixed. Thermal-hydraulic data so obtained are used as boundary convection conditions in the thermal analyses.

The model used for these ones is representative of the slice between two horizontal cooling plates, placed at the middle between two vertical plates, insofar the influence of these ones on thermal behaviour can be neglected. Three U-tubes are modeled as shown in the figure 5.

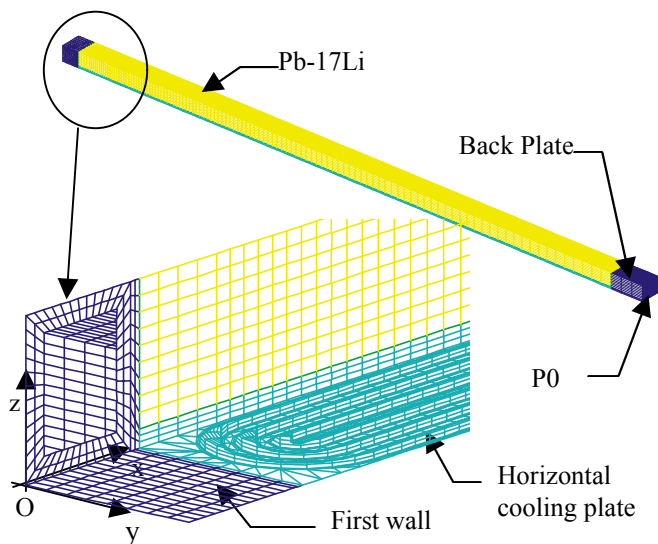


Figure 5 : Model used for thermo-mechanical analyses

In order to carry-out conservative study, it has been assumed that the He bulk temperature in the FW is equal to the maximum one (at FW outlet) and that in the BZ it follows the profile obtained with the FIDAP thermal - hydraulic code, adapted to the inlet and outlet temperature values previously estimated [2]. Although this profile is related to a model smaller in the radial direction and to the power density of the DEMO WCLL reactor, it can be preliminarily supposed that its trend should not change. In particular, it was assumed that the He temperature reaches its maximum value, which is almost 30 °C higher than the outlet one, at 15 cm from the FW. This is why, in this concept, the outlet He temperature was limited to 470°C instead of the foreseen 500°C target. As shown below, this reduction is mandatory to fulfill design limits.

The considered thermal loads were a uniform surface heat flux on the FW of 0.5 MWm⁻² and a nuclear heat deposition profile from [9], with a maximum power density of 16.5 Wcm⁻³ on the Pb-17Li and 17 Wcm⁻³ in the Eurofer. Main optimized thermal-hydraulic parameters are summarized in the table 1. Maximum, average and minimum temperature values in various materials of the model region are summarized in table 2.

Table 2 : Temperature ranges in the blanket materials

	T _{max} (°C)	T _{ave} (°C)	T _{min} (°C)
FW steel	521	436	376
BZ steel	542	457	367
Pb-17Li	662	478	372
Steel/Pb-17Li interf.	542		

In the FW, steel temperature reaches a maximum of 521°C, keeping a comfortable margin (35°C) to the assumed limit. As expected the maximum is located in the region in the front of the plasma. In the BZ, steel temperature reaches 542°C, in the zone where the He bulk T is the highest. 542°C is also the maximum temperature at the interface between the steel and the liquid metal. In previous WCLL studies, 480°C was considered as the limiting value due to corrosion. The choice to have high He outlet temperature (500°C) being not compatible with this limit, further R&D has been launched in order to assess the behaviour of this interface at higher temperatures. Sensibility studies showed that temperature profile in the steel strongly depends on the He bulk temperature profile. Further thermal-hydraulic detailed analyses (with appropriate codes) should be, thus, needed in order to better take into account this bridge phenomenon.

Thermo-mechanical results

Thermo-mechanical analyses have been performed in the above-described model, both in nominal and in faulted conditions. The procedure and the criteria used for the analyses relies on the RCCMR [7], DISDC [8] design rules. In this report, in accordance with the RCC-MR rules, elastic analysis was the method employed. Moreover, the octahedral shear stress (or Von Mises) method was used for determine the stress intensity.

The following loads and boundary conditions have been taken into account:

- Thermal field obtained with thermal analysis.
- Internal pressure on the FW and BZ channels (8 MPa).
- Internal pressure on the box and CP surfaces in contact with the liquid metal. In nominal conditions, this pressure has been assumed equal to 1 MPa (hydrostatic pressure and pressure drops); in faulted conditions it has been assumed that all box will be pressurized at 8 MPa.
- The plane Ox Oy is a symmetry plane.
- The plane Ox Oz is a symmetry plane.
- The point P0 is clamped.
- The points on the other planes are assumed to have uniform displacements in the direction normal to their lying plane.

Table 3 summarizes maximum Von Mises stress (split in primary and total) values (MPa) in normal and faulted conditions (NC/FC) and compares them with corresponding limits.

Table 3 : Primary and total VM stresses and margin to the corresponding limits (MPa) in the FW and in the CPs

	FW		Cooling plates	
	VM	Marg.	VM	Marg.
Primary NC	55	80	55	70
Total NC	269	90	300	100
Primary FC	101	140	201	64

As shown in the table, RCC-MR criteria are everywhere met, thus the limiting point of this concept remains the maximum temperature in the steel and at the interface between the steel and the liquid metal.

CONCLUSION

The main drawback of the concept using horizontal cooling of the BZ with U-tubes remains the bridge effect between hot and cold leg of the cooling channels. The He temperature reaches a value higher than the outlet one and this maximum is located in a region where the power density in the BZ is high. Due to this and in order to fulfill design criteria, the He outlet T must be reduced to 470°C instead of the 500°C initially foreseen to maximize the reactor conversion cycle efficiency. In addition, critical issues appeared on the design of the He collector/connection system that would require further improvement/modifications of the concepts. This will be the subject of the next design development activities. This further activity will also be intended to optimized the He flow layout to maximize the acceptable He outlet temperature.

REFERENCES

- [1] S. Hermsmeyer et al., Improved Helium Cooled Pebble Bed Blanket, FZK Report, FZKA 6399, December 1999.
- [2] S. Hermsmeyer, personal communication.
- [3] M. Küchle, Material Data base for the NET Test Blanket Design Studies, Kernforschungszentrum Karlsruhe, February 1990.
- [4] F. Tavassoli, DEMO Interim Structural Design Criteria, DISDC, Appendix A Material design limit data A3.S18 Modified 9Cr-1Mo Steel, Interim SM 5.1 report CEA/CEREM/DECM, September 1999.
- [5] S.J. Zinkle J.P. Robertson, R.L. Kluch, Thermophysical and mechanical properties of Fe-(8-9)%Cr reduced activation steels (4/25/98 draft) ORNL.
- [6] A. Kohyama A. Hishinuma, D.S. Gelles, R.L. Klueh, W. Dietz, K. Ehrlic, Low activation ferritic and martensitic steels for fusion application, Fusion Reactor Materials, 233-237 (1996) 138.
- [7] RCCMR Règles de Conception et de Construction des Matériels mécaniques des îlots nucléaires Rapides, French design and construction rules for fast breeder reactor power stations, AFCEN (ed. 1985).
- [8] F. Tavassoli, DEMO Interim Structural Design Criteria, DISDC, Appendix A Material design limit data, A.GEN: General, Interim SM 5.1 Report, CEA/CEREM/DECM, September 1999.
- [9] Y. Chen, U. Fischer, P. Pereslavytsev, F. Wasastjerna, The EU Power Plant Conceptual Study - Neutronic Design Analyses for Near Term and Advanced Reactor Models" FZK Report, FZKA-6763P, June 2002.

REPORTS AND PUBLICATIONS

Y. Poitevin, A. LI Puma, M. Eid; G. Rampal, Design conceptual studies of a Helium-Cooled Lithium-Lead Breeding Blanket, CEA Report, SERMA/RT/02/3191/A.

TASK LEADER

Antonella LI PUMA

DEN/DM2S/SERMA
CEA Saclay
91191 Gif-sur-Yvette Cedex

Tél. : 33 1 69 08 79 76
Fax : 33 1 69 08 99 35

E-mail : alipuma@cea.fr

Task Title: BLANKET NEUTRONIC INSTRUMENTATION[illegible]

INTRODUCTION

[illegible]

The neutronic instrumentation of the Test Blanket Modules (TBM) appears to be a key point of the TBMs Test Program in ITER, since it will contribute to validate the performances of the blanket in term of tritium production (a good evaluation of the neutron flux is fundamental for estimating the tritium production and thus making a relevant tritium balance in the TBM).

A neutronic instrumentation has to be assessed, taking into account specific constraints of Breeding Blankets (operating conditions, magnetic field, geometry,...).

In this objective, DSM/DRFC (Mr. Gilles MARTIN) and DEN/DER collaborated in 2001 and 2002, for carrying out an experimental program in TORE SUPRA with standard fission chambers.

SUMMARY OF 2001 ACTIVITIES

Preliminary experimental tests with a CFUE24 fission chamber (manufactured by the Photonis company) were carried out in TORE SUPRA facility in 2001, in order to qualify its operation in an intense magnetic field and under plasma atmosphere.

It was the first time that such a detector was used in a field higher than 1 Tesla.

The main characteristics of the CFUE24 are as follows:

- external diameter: 7 mm
- material of the electrodes: stainless steel
- fissile material: uranium enriched in ^{235}U (93 %)
- mass of uranium: ≈ 16 mg
- filling gas: argon with N_2 (4 %) ; $P = 900$ kPa
- thermal neutrons sensitivity: $\approx 10^{-2}$ c.s $^{-1}$ /n.cm $^{-2}$.s $^{-1}$
- cable: \varnothing 6 mm (stainless steel and alumina)

The CFUE24 operated in an average magnetic field from 1.6 up to 2.3 T, with a longitudinal gradient up to 8 T/m. The direction of the magnetic field was perpendicular to the axis of the chamber.

The temporal evolution of the counting rate is given on the figure 1 : the signal of the CFUE24 located in the magnetic field of 2.3 T follows correctly the counting rate of a CFUL01 fission chamber located outside the facility where the magnetic field is weak (< 0.1 T).

A statistical study between the total number of counts given by the two fission chambers is presented on the figure 2.

These curves were obtained with different conditions of plasmas and instantaneous counting rates and show a nearly perfect linearity between the two detectors.

These tests carried out in TORE SUPRA in 2001 showed that a fission chamber provided a normal counting rate in a magnetic field up to 2.3 T, close to the fusion plasma (roughly 30 cm).

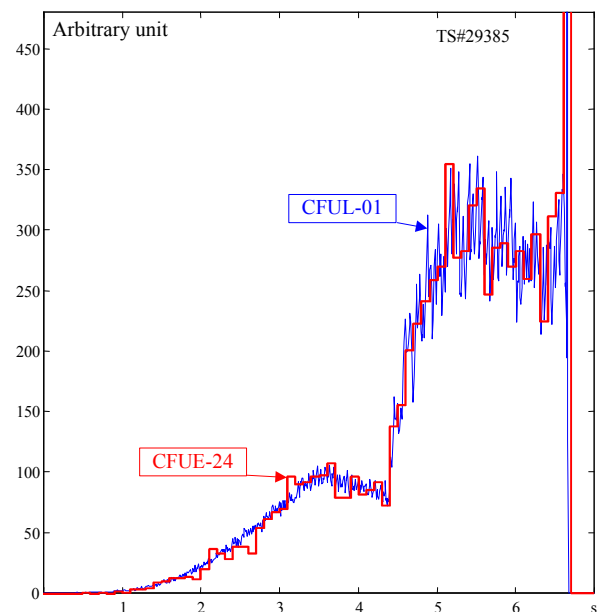


Figure 1 : Temporal evolution of the counting rate
of 2 fission chambers:
CFUE24 ($B = 2.3$ T), CFUL01 ($B < 0.1$ T)

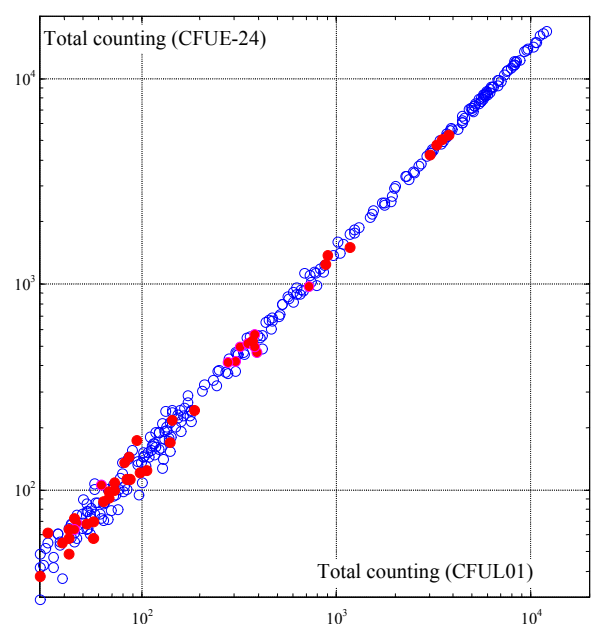


Figure 2 : Comparison of total counting
(hollow symbol: $B = 2.3$ T ; full symbol : $B = 1.6$ T)

2002 ACTIVITIES

[illegible]

The objective of the 2002 tests was to continue the study of the behaviour of fission chambers up to 5 Tesla.

Two fission chambers (CFUE24, CFUM11) and a californium source were located in a block made of polyethylene (dimensions : about 25 x 25 x 25 cm).

This device was fixed on the internal wall of TORE SUPRA facility, with two possible positions :

- magnetic field at 45° relative to fission chambers axis,
- magnetic field parallel to fission chambers axis.

The CFUE24 is already presented on the previous page and the main characteristics of the CFUM11 (also manufactured by the Photonis company) are as follows:

- external diameter: 25.4 mm
- material of the electrodes: aluminium
- fissile material: uranium enriched in ^{235}U (93 %)
- mass of uranium: ≈ 150 mg
- filling gas: argon with N_2 (4 %) ; $P = 400$ kPa
- thermal neutrons sensitivity: $\approx 10^{-1} \text{ c.s}^{-1}/\text{n.cm}^{-2}.\text{s}^{-1}$
- cable: FILECA 1209 (Cu, Ag and polyethylene)

This experiment was carried out without plasma discharges. The temporal evolution of the counting rates is given on the figure 3 and on the figure 4 : the signals of the detectors were recorded only during the magnetic fields changes (slope = 0.2 to 0.25 T/mn).

The fluctuations of the counting rates is due to statistical effects (integration range = 8 s).

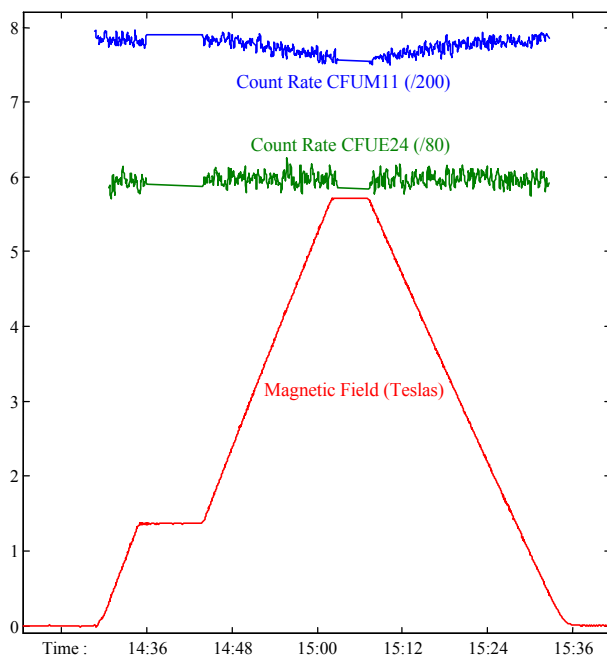


Figure 3 : First experiment :
Magnetic field at 45° relative to the fission chambers axis

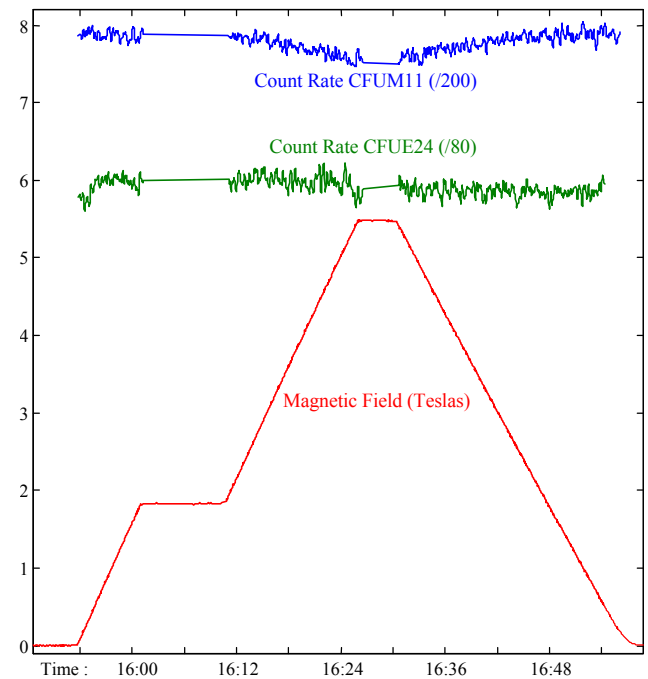


Figure 4 : Second experiment :
Magnetic field parallel to the fission chambers axis

The figure 5 and the figure 6 represent the counting rates according to the magnetic field intensity (B).

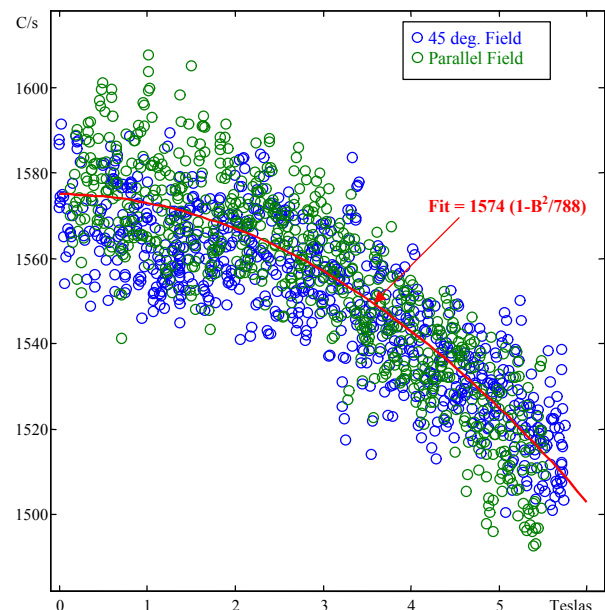


Figure 5 : CFUM11 fission chamber :
Count rate versus magnetic field strength

The CFUE24 seems almost unaffected by the strength of the magnetic field (maybe a small trend to rise).

On the other hand, the sensitivity (S) of the CFUM11 decreases approximately 5 % for B = 5.6 T. For B = 0 T up to 6 T, and under our specific experimental conditions (californium neutron source, no plasma,...), we can assume that S is correctly described by the parabolic function as follows :

$$S(B) = S(0) \cdot (1 - \frac{B^2}{788})$$

This physical effect is only observed for the CFUM11 probably because the strength of the electric field used to collect the charges is stronger in the CFUE24 than in the CFUM11, due to its smaller size (polarisation voltages are of the same magnitude).

Considering the figure 5 and the figure 6, both fission chambers are not sensitive to the direction of the magnetic field relative to their longitudinal axis.

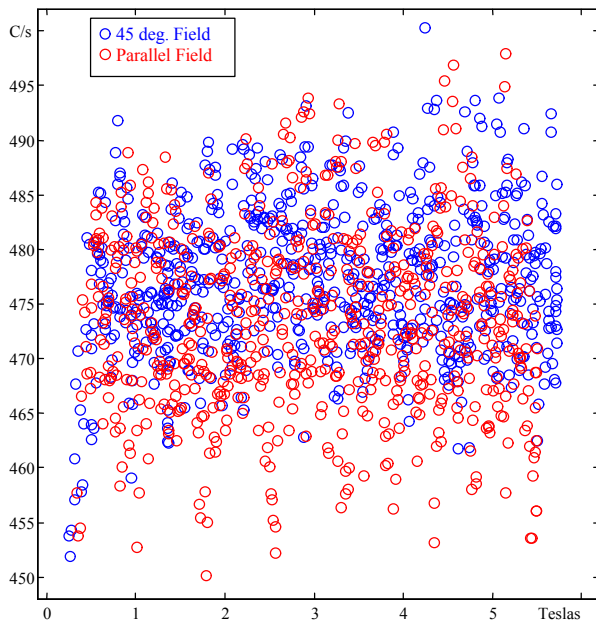


*Figure 6 : CFUE24 fission chamber :
Count rate versus magnetic field strength*

TASK LEADER

Christophe BLANDIN

DEN/DER/SPEX/LPE
CEA Cadarache
13108 Saint Paul Lez Durance Cedex

Tél. : 33 4 42 25 48 04

Fax : 33 4 42 25 78 76

E-mail : christophe.blandin@cea.fr

CONCLUSIONS

From these preliminary tests in TORE SUPRA facility, the main following conclusions can be drawn:

- standard fission chambers provide normal counting rates in a magnetic field up to 2.3 T during plasma discharges ;
- standard fission chambers can be used in a magnetic field up to 5.6 T (experiment carried out with a californium source, thus without plasma), even if a loss of sensitivity (5 %) was observed for the CFUM11 (external diameter = 25.6 mm) ; thus the smallest fission chamber possible (but sensitive enough) has to be selected for the instrumentation of the Test Blanket Module (TBM) ;
- the optimized fission chamber (size, nature fissile material, filling gas, ...) and its associated cable (as low sensitive to magnetic field as possible) will have to be defined in the future years and of course, to be tested in the expected operating conditions in the TBM.

Task Title: HELIUM COMPONENTS TECHNOLOGY
Problems and outlines of solutions

INTRODUCTION

In the HCLL (Helium Cooled Liquid Lead) concept, helium in gaseous state is used for cooling the blankets, and the divertor.

Helium is studied as a coolant in fusion reactors for many reasons. It is a gas which does not change phases over a wide temperature range, which eliminates drastic modifications in the thermal transfer. It is a very efficient exchange agent among gases (only hydrogen is better). It is compatible at all temperatures with all materials. It is transparent to neutrons, and is only slightly activated under radiation (only isotope ^3He , present in minute proportions, can form tritium). Lastly, helium, with a liquefaction temperature lower than that of all gases (4.35 K), is easy to purify using cryogenic means.

This task is devoted to the identification and resolution of technological problems raised by helium at pressures of about 80 bars, and with temperatures locally up to 800°C.

2002 ACTIVITIES

The purpose of the 2002 activity was to list the generic technological problems encountered when using high temperature and pressure helium circuits, from the view point of fusion reactor shields, blankets and divertors, and to propose an outline of possible solutions. This study is based on the feedback from gas cooled reactors and experimental loops, which have existed or which are still under project form.

The components and subjects addressed to are : hot gas pipes under pressure, heat exchangers, isolating components (valves), circulators, helium storage system, helium quality control, graphite (if any) oxydation, non nuclear instrumentation.

Two types of problems due to the type of fluid itself were mentioned:

- the extreme volatility of helium favors its leakage, especially at the weak points which are the section elements and the seals. From a tightness point of view, the technology of circulators is a problem, especially for large flow rates,
- this gas, if pure, does not allow the presence of oxide layers which would lessen the friction of metallic parts.

Moreover, there are problems due to temperature and pressure levels (500°C to 800°C, 50 to 80 bar), but they are within the temperature and pressure ranges used in gas cooled fission reactors (use of gas from 300°C to 1000°C, 30 bars to 100 bars).

These levels of temperature and pressure mostly raise the problem of thermal barriers. The fact should also be mentioned that precautions might be necessary to stop the measurements in temperature during transients from being disturbed, because of the thermal radiation exchanges between the thermocouple and the wall.

Lastly, a system of control for the chemical and radio-chemical quality of helium and leak detection systems must be foreseen.

CONCLUSION

The solutions found or under development for the gas reactors should be adapted with a minimum of effort to the case of the helium cooling circuits of the protective shields, blankets and divertor of fusion reactors.

REPORTS AND PUBLICATIONS

J.L. Berton et al. « Identification of technological problems linked to helium circuits and proposals for solutions ». CEA Report NT DER/ STR/LCET 02/034.

TASK LEADER

Jean-Luc BERTON

DEN/DER/STR/LCET
CEA Cadarache
13108 Saint Paul Lez Durance Cedex

Tél. : 33 4 42 25 77 93
Fax : 33 4 42 25 66 38

E-mail : jean-luc.berton@cea.fr

UT-TBM/MAT-LM/MAG

Task Title: LIQUID METAL CORROSION UNDER MAGNETIC FIELD

INTRODUCTION

Corrosion of materials exposed to liquid metal depends on many parameters such as temperature, hydrodynamics, thermal gradient... In the high magnetic field confining the plasma, the flow of the liquid alloy is characterized by the presence of a core velocity in the central region and various boundary layers in the vicinity of the channel-walls which exhibit a strong velocity gradient.

When the mass transfer between a solid and a liquid is controlled by the velocity gradient at the wall, a modification of the corrosion process may thus be expected in the presence of the magnetic field. It is important to study this phenomenon and quantify the effect of the field on the corrosion of steels in contact with the Pb-17Li alloy.

For this purpose, it has been proposed to perform corrosion tests in Pb-17Li under magnetic field in flows driven by a rotating disk inside a cavity. Such a study is of interest because the hydrodynamics in this configuration can be well described by numerical simulation and thus the influence of the field on the mass transfer can be well characterized. The work already performed has allowed to design the experimental device (a rotating disk inside a cylindrical crucible) and to characterise the liquid hydrodynamics [1-3].

In 2002, corrosion tests of an austenitic and a martensitic steel in liquid Pb-17Li were performed without and under a magnetic field with a flow generated in a cylindrical cavity by a rotating disk with a controlled hydrodynamic.

2002 ACTIVITIES

EXPERIMENTAL

The experiment (figure 1) is based on the fluid motion generated by a rotating disk. The Pb-17Li alloy is contained in a cylindrical crucible made of the austenitic steel, which has been aluminised to prevent it from corrosion. The rotating disk, which is the specimen to study, constitutes the upper part of the crucible.

The crucible is heated with an electrical furnace composed of two heating elements allowing to produce a stable temperature gradient between its top (480°C or 510°C) and its bottom (410°C or 440°C).

To avoid Pb-17Li oxidation, argon is continuously delivered at a small flow rate above the top of the crucible. The device can be placed inside the solenoid which allows to impose a longitudinal magnetic field, continuously adjustable between 0 and 0.5 Tesla.

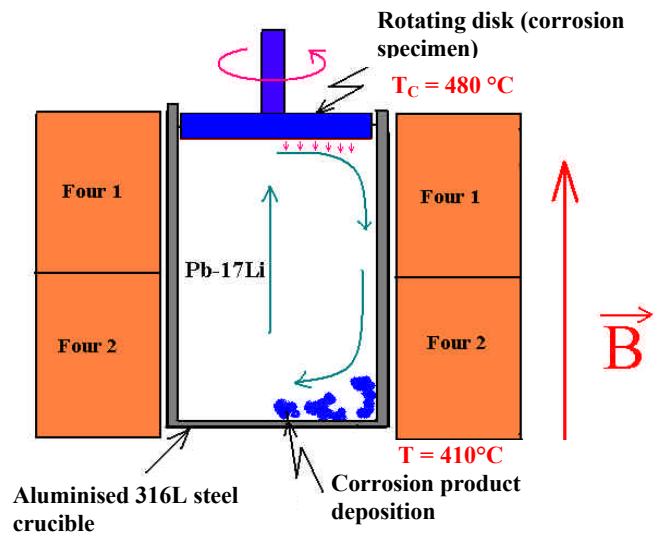


Figure 1 : Presentation of the device

In order to avoid the corrosion of the upper part of the rotating disk, this latter has also been aluminised. But the aluminised coating of the disk face in contact with Pb-17Li was mechanically removed. As it was not possible to coat the T91 martensitic steel rotating disk, thus a 1 mm thick disk was maintained by a clip to an aluminized 316L austenitic steel rotating disk. A view of the specimens is given in figure 2.

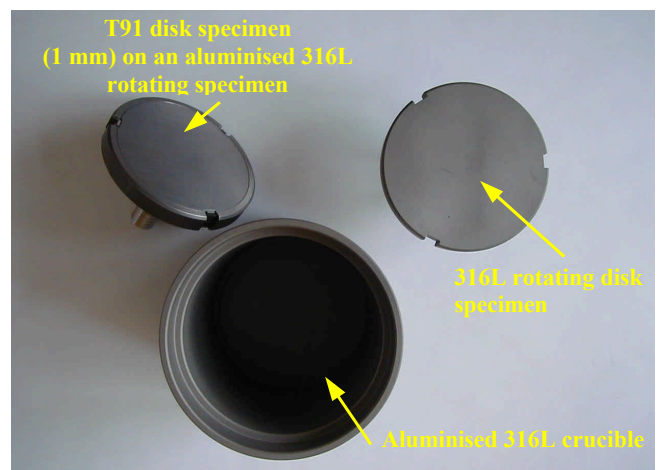


Figure 2 : Pictures of the rotating disk specimen and crucible

All the operations required to introduce the rotating disk and the liquid Pb-17Li in the crucible were carried out in a glove box with purified argon gas to prevent air contamination.

In a first step, the rotating disk was placed at the bottom of the crucible and all was heated in a furnace at 350°C. The Pb-17Li was melted in another furnace and the liquid was poured into the crucible.

The space between the crucible and the rotating disk (about 1 mm) is such that it allows the liquid Pb-17Li to flow through. At the end, the rotating disk floats on the liquid Pb-17Li at the top of the crucible. About 800 g of Pb-17Li were introduced into the crucible corresponding to about 600 mm Pb-17Li height. After cooling, the crucible with rotating disk was introduced into the device in the container closed at its top by a cover supporting the motor. This equipment was sent to the LEGI laboratory to perform the corrosion test without or under magnetic field. After test and cooling, the device was sent to CEA and the rotating disk was removed from Pb-17Li. The remaining Pb-17Li adhering to the specimen surface was then removed by immersing the specimen in an alcohol, acetic acid and hydrogen peroxide mixture. Then, the observations to characterise the corrosion were performed. The experimental conditions of the tests are given in table 1.

RESULTS

Corrosion results of 316L austenitic steel

Weight measurements of the specimens do not lead to significant values due to the difficulty to totally remove the remaining Pb-17Li adhering to the surface. The disk thickness measured at different places before and after tests do not show variations, taking into account the uncertainty of the micrometer gauge (10 μm). The observations and analyses performed on the cross-section of the two disks along their surface show a corrosion layer made of metallic particles with a network of channels full of Pb-17Li (figure 3). The chemical composition of the corrosion layer is the same all along the surface of each disk (without and under a magnetic field) and corresponds to Fe (90 wt%), Cr (about 7 wt%) and Mo (3 wt%). The observations show that, for each specimen, the corrosion layer thickness increases from the centre to the disk extremity. From figure 4, we can see that:

- In the two cases, the thickness variations with the distance to the specimen centre are not regular.
- At a same distance from the centre, the corrosion layer thickness is smaller on the specimen tested under a magnetic field.

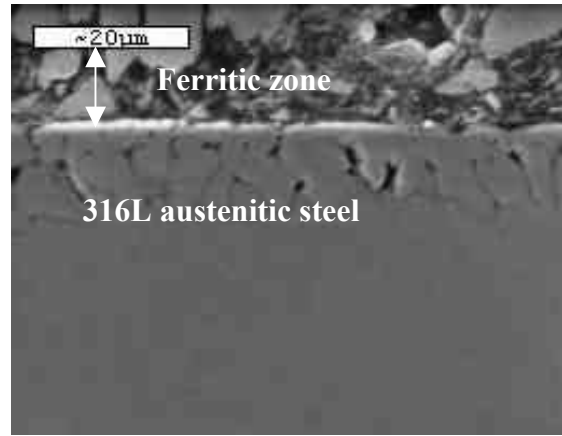


Figure 3 : Cross-section micrograph of 316L austenitic steel at the extremity of the rotating disk after 350 h at 480°C under magnetic field in liquid Pb-17Li, ($W = 2.1 \text{ rad.s}^{-1}$, $R_e = 21000$, $H_a = 130$)

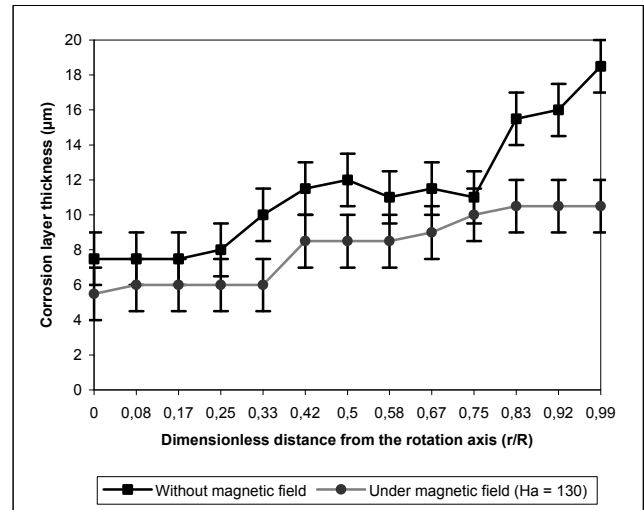


Figure 4 : Thickness of the porous ferritic corrosion layer of the 316L austenitic steel rotating disks along the dimensionless radial coordinate r/R after 350 h at 480°C without and under a magnetic field

Table 1 : Experimental conditions of the tests without and under a magnetic field

Steel	Temperature of the specimen T_c	Temperature of the crucible bottom T_f	Hartman number H_a^{**}	Ω (rad.s^{-1})	Reynolds number Re^*	Duration (hours)
316L austenitic steel	480 °C	410 °C	$H_a = 0$	2.1	21000	350
	480 °C	410 °C	$H_a = 130$, $k=0.1$	2.1	21000	350
T91 martensitic steel	510 °C	440 °C	$H_a = 0$	2.1	21000	500
	510 °C	440 °C	$H_a = 200$, $k=0.042$	2.1	21000	500

*: $Re = \Omega R^2 / \nu$ with $R = 30 \text{ mm}$

** : $H_a = B_0 R (\sigma_f / \eta \nu)^{1/2}$ with $B_0 = 0.2 \text{ tesla}$

Corrosion results of T91 martensitic steel

The weight variation of the rotating disk tested without magnetic field ($\Delta m = -0.03284$ g) is more important than under a magnetic field one ($\Delta = -0.024689$ g). Assuming an homogenous dissolution all over the disk surface, the mean thickness losses correspond to $1.5 \mu\text{m}$ and $1.2 \mu\text{m}$ respectively without and under magnetic field.

The uncertainties of the geometrical measurements are too high to detect thickness variations due to the corrosion.

The observations and analyses performed on the cross-section of the two specimens along their surface show a homogeneous dissolution without formation of a superficial corrosion layer and intergranular attack.

Only a weak increase in the surface roughness was observed but microprobe analysis did not show any chromium or iron depletion near the surface.

DISCUSSION

Corrosion mechanisms

The nature and the morphology of the corrosion layer at the surface of the 316L austenitic steel specimens after these tests are very similar to the results previously observed by others [4] who report the formation of a superficial ferritic porous layer due to the preferential dissolution of Ni and Cr. As previously observed [5], [6], the presence of a magnetic field does not modify the corrosion layer chemical composition.

N. SIMON [7] has proposed a mechanism for the corrosion of 316L austenitic steel in an isothermal liquid Pb-17Li. The first step is the Ni and Cr superficial dissolution, followed by a phase transformation of the austenitic matrix into ferrite with the formation of porosities. Finally, the diffusion of dissolved species into the porosities filled by some liquid metal and into the diffusion boundary layer of liquid Pb-17Li occurs.

The limiting step of this process is the Cr dissolution into the liquid when the corrosion layer thickness is small compared to that of the diffusion boundary layer. At the opposite, the diffusion limitation is in the porosities when the layer becomes thick compared to the diffusion boundary layer.

The corrosion of T91 martensitic steel without and under a magnetic field is characterized by an homogeneous dissolution without formation of a superficial corrosion layer. No intergranular attack and preferential dissolution have been observed by our analytical techniques. This corrosion behaviour corresponds to what has been observed in different experiments [5], [6].

Influence of the hydrodynamic flow

An hydrodynamic model of the liquid flow in the experimental device has been previously developed [3]. Compared to the classical rotating disk, it takes into account the finite dimensions of the device.

The convective diffusion of a dissolved element can be described by the following equation, taking into account the hydrodynamic model:

$$u_r \frac{\partial C}{\partial r} + \frac{u_\theta}{r} \frac{\partial C}{\partial \theta} + u_z \frac{\partial C}{\partial z} = D \left(\frac{\partial^2 C}{\partial r^2} + \frac{1}{r} \frac{\partial C}{\partial r} + \frac{\partial^2 C}{\partial z^2} + \frac{1}{r^2} \frac{\partial^2 C}{\partial \theta^2} \right) \quad (1)$$

where C is the dissolved element concentration, and r , z , θ are the cylindrical coordinates.

If the Cr diffusion in the boundary layer is considered as the limiting step of the 316L steel corrosion process, in the steady state and assuming:

- an axial symmetry
- the Cr solubility is achieved at the rotating disk
- the Cr concentration is zero at the other walls

the calculated mass flux at the rotating disk is defined through the classical Sherwood number

$$sh(r) = \frac{\text{Flux}(r)}{S_C C_{\text{ref}}} \quad \text{Where } \text{Flux}(r) = -\frac{1}{Sc} \frac{\partial C}{\partial z} \quad \text{and } C_{\text{ref}} = 1 \quad (2)$$

In these conditions, from this model, it is expected a constant corrosion amplitude all along the disk. It is different from experimental results obtained with the 316L steel.

The increase of corrosion at the disk extremity can be explain by instabilities which can arise near the lateral wall. Elsewhere, the corrosion amplitude variations are not yet explained: they could be due to a change in the corrosion limiting step or by the presence of the porosities in the corrosion layer.

Concerning the T91 martensitic steel, it has already been shown that the corrosion limiting step in turbulent flowing Pb-17Li is the diffusion of dissolved Fe in the boundary layer. Assuming that it is also true in our experimental conditions, we can calculate the T91 martensitic corrosion rate using the Levich equation for a rotating disk in an infinite system [8]:

$$V_{\text{corrosion}} = 0.620 D^{2/3} \omega^{1/2} \nu^{-1/6} C_s \quad (3)$$

With D : diffusion coefficient of Fe in Pb-17Li ($\text{m}^2 \cdot \text{s}^{-1}$), ω : angular velocity of the rotating disk ($2.1 \text{ rad} \cdot \text{s}^{-1}$), ν : Pb-17Li kinematic viscosity ($\nu = 1.74 \cdot 10^{-7} \text{ m}^2 \cdot \text{s}^{-1}$) and C_s : dissolved Fe concentration ($\text{g} \cdot \text{m}^{-3}$).

If we take for $C_s = 47.5 \text{ ppm} = 493.52 \text{ g} \cdot \text{m}^{-3}$ and $D = 2 \cdot 10^{-14} \text{ m}^2 \cdot \text{s}^{-1}$ the values determined by V. Coen [9] and T. Dufrenoy [10] respectively, we obtain $e_{\text{corrosion thickness}} = 1.6 \mu\text{m}$. For the values given by F. Feuerstein [11] which are $C_s = 0.542 \text{ ppm} = 5.63 \text{ g} \cdot \text{m}^{-3}$ and $D = 7.46 \cdot 10^{-11} \text{ m}^2 \cdot \text{s}^{-1}$ we have $e_{\text{corrosion thickness}} = 2.7 \mu\text{m}$. These values are close to the experiment measure ($e_{\text{corrosion thickness}} = 1.7 \mu\text{m}$ without magnetic field). Thus, it seems that the limiting step of the T91 martensitic steel corrosion in laminar flowing is the diffusion of dissolved Fe in the boundary layer.

Influence of the magnetic field

The corrosion layer thickness on the 316L austenitic steel disk tested under a magnetic field is always thinner than the one developed on the specimen tested without magnetic field. This is due to the fact that the meridian flow governed by u_r and u_z is smaller under a magnetic field, these two flow velocity components being also lower. This confirms the action of the magnetic field through the hydrodynamics on corrosion. However, the shape of the corrosion depth profile along a radius has to be explained. We can only point out that the trays are at the same distances from the axis in the two cases (without and under magnetic field). The same type of phenomena are expected with the T91 martensitic steel.

CONCLUSION

The 316L austenitic steel and T91 martensitic steel corrosion experiments in the presence of Pb-17Li with a rotating disk in a cylindrical cavity have been performed without and under a magnetic field (parallel to the rotation axis). Numerical calculations of the velocity fields and mass flux in the cavity have been done in order to explain the corrosion results.

The morphology and the nature of the corrosion 316L austenitic steel after tests are the same without and under a magnetic field. In the tested conditions, the corrosion process is probably limited by the Cr convective diffusion and depends on the meridional flow velocity components in the hydrodynamic boundary layer. It explains why the magnitude of the corrosion is in the present experiment smaller in the presence of the magnetic field. A full understanding could require the integration of the porous corrosion depth in the model.

The T91 experiments have confirmed the smaller mass transfer in presence of magnetic field in the tested conditions. The corrosion process is probably limited by the Fe convective diffusion. However, the magnitude of the corrosion is too small to allow to measure a variation of corrosion depth along the disk.

REFERENCES

- [1] F. Barbier, A. Alemany and A. Kharicha, Corrosion in moving liquid Pb-17Li under magnetic field: Hydrodynamic modeling in rotating flows, CEA report, RT-SCECF 510 (December 1999).
- [2] A. Kharicha, A. Alemany and F. Barbier, Influence of the magnetic field and the conductance ratio on the hydrodynamic of a fluid driven by a rotating disk in a cylindrical enclosure, Proceedings of the 4th International PAMIR Conference on Magneto-hydrodynamic at Dawn of Third Millennium, Presqu'île de Giens, France, September 18-22, 2000, 1 (2000) 405-410.
- [3] F. Barbier, A. Alemany and A. Kharicha, Hydrodynamics in liquid metal flow driven by a rotating disk under magnetic field: experiment and simulation, CEA report, RT-SCECF 545 (November 2000).
- [4] T. Flament, P. Tortorelli, V. Coen, H. U. Borgstedt, Compatibility of materials in fusion first wall and blanket structures cooled by liquid metals, J. Nucl. Mat. 191-194 (1992) 132-138.
- [5] T. Flament, A. Terlain, J. Sannier, P. Labbé, Influence of magnetic field on thermohydraulic and corrosion in the case of the water-cooled blanket concept, Fusion Technology 1990, B. E. Keen, M. Huguet, R. Hemsworth (editors), Elsevier Science Publishers B. V., (1991), 911-915.
- [6] A. Terlain, T. Dufrenoy, Influence of a magnetic field on the corrosion of austenitic and martensitic steels by semi-stagnant Pb-17Li, J. Nucl. Mater. 212-215 (1994) 1504-1508.
- [7] N. Simon, A. Terlain, T. Flament, The compatibility of austenitic materials with liquid Pb-17Li, Corrosion Science, 43 (2001) 1041-1052.
- [8] Levich, Physicochemical hydrodynamics.
- [9] V. Coen, T. Sample, Pb-17Li: a fully characterized liquid breeder, Fusion Technology 1990, Proc. 16th SOFT, 248-252 (1990).
- [10] T. Dufrenoy, V. Lorentz, A. Terlain, Determination of diffusion coefficient of iron in liquid alloy, RT-SCECF 520, December 2000.
- [11] H. Feuerstain, H. Gräbner, J. Oschinski, J. Beyer, S. Horn, L. Höner, K. Santo, Compatibility of 31 metals, alloys and coatings with static Pb-17Li eutectic mixture, Forschungszentrum Karlsruhe, FZKA 5596 (1995).

REPORT

Ph. Deloffre, A. Terlain, A. Alemany, A. Kharicha, Corrosion study of an austenitic steel in Pb-17Li under magnetic field and rotating flow, CEA report, To be issued.

TASK LEADER

Philippe DELOFFRE

DEN/DPC/SCCME/LECNA
CEA Saclay
91191 Gif-sur-Yvette Cedex

Tél. : 33 1 69 08 16 14
Fax : 33 1 69 08 15 86

E-mail : philippe.deloffre@cea.fr

UT-TBM/MAT-LM/Refrac

Task Title: COMPATIBILITY OF REFRACTORY MATERIALS WITH LIQUID ALLOYS

INTRODUCTION

High flux components in a fusion reactor will be submitted to high thermal flux and to high temperatures. Liquid metals and in particular liquid eutectic Pb-17Li, due to their high conductivity are good candidates for removing such high heat flux. However, it is well known that liquid metals can be very corrosive at high temperatures. It is therefore necessary to assess the corrosion behaviour of high flux component materials in contact with liquid metals. As far as the constitutive materials of these components are concerned, tungsten alloys appear to be the best choice.

In a previous study, in a first step, it has been shown that no corrosion of tungsten occurs at 800°C for 1500 hours in static isothermal Pb-17Li [1]. In a second step, the corrosion of tungsten by Pb-17Li in the presence of a thermal gradient (800°C maximum temperature and a 60°C thermal gradient) and a very low liquid flow velocity has been studied: in the tested conditions no corrosion of tungsten has been observed [2].

Concerning the interaction between tungsten material and liquid Pb-17Li, it is expected that dissolution can occur. When the corrosion proceeds by dissolution, the solubility of the dissolved species has a large influence on the corrosion rate.

Concerning the solubility of W in Pb-17Li, only a few experiments were performed with W-crucibles and no reliable information on the solubility of tungsten in Pb-17Li exist and it is very important to determine them. A special device has been previously designed to perform such measurements. In 2002, solubility of tungsten in Pb-17Li has been determined at 800°C and 1000°C.

2002 ACTIVITIES

EXPERIMENTAL

The device for the determination of the metallic species solubility in Pb-17Li has been previously designed and tested [2]. It consists of (see figure 1):

- A crucible made of TZM: its size has been chosen not too large to recover all the Pb-17Li after the experiment in order to analyse it and to avoid any thermal gradient which can induces mass transfer and not too small to put in contact with Pb-17Li a sample with a sufficient surface area to favour the dissolution process. This crucible has a TZM holder welded to the cover.

On this holder are fixed at the bottom the sample and at the top a little TZM crucible to in-situ sample some Pb-Li by turning upside-down and coming back the container with the crucible for chemical analysis and determining the amount of dissolved elements. The advantages of this sampling system are: first the sample is no longer in contact with the specimen, second it is sufficiently small to be totally analysed and finally it avoids all the uncertainties linked to the possible segregations when a freeze sample is only partially analysed. The cover is welded to the crucible under vacuum by electron beam technique.

- A container made of alloy 601 in which is the crucible. The container is closed by welding (by electron beam technique) a cover made of the same material. The aim of this container avoids the excessive oxidation by air of the TZM crucible during the experiment.
- A furnace in which is placed the container.

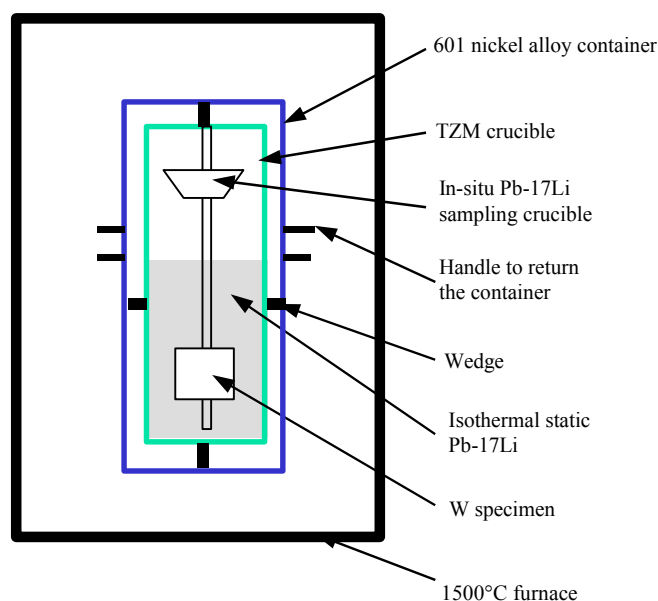


Figure 1 : Schematic drawing of the device for solubility measurements

The procedure to perform a test is the following: the container, the crucible, the cover and the holder are heated up to 500°C for 24 hours under vacuum. Moreover, a specimen is washed with a alcohol, acetone and tetrachloroethylene mixture and after with alcohol and then dried. Then, in a glove box with a purified argon atmosphere, the crucible is filled with liquid Pb-17Li. The holder with the sample is immersed in the liquid and the cover is mounted. The crucible is ready to be closed by welding the cover.

After, the closed crucible is placed in the container which is also closed by welding.

The container is then placed in the furnace and heated up to the experiment temperature.

During the test, the container is periodically shaken in order to mix Pb-17Li.

At the end of the experiment, at the test temperature, the container was turned upside down (in-situ sample Pb-17Li) and cooling.

The container and the crucible were open. In the glove box, the Pb-17Li sample was recovered and the Pb-17Li melted for removing the tungsten specimen.

Sintered polycrystalline tungsten has been supplied by Plansee. It has been used as small platelets 10 mm x 5 mm x 1 mm with the as received surface state. Pb-17Li from Métaux Spéciaux has been used for these experiments.

RESULTS

Four tests have been performed: one at 800°C and three at 1000°C.

The Pb-17Li amount put into each crucible is between 40 and 45 g. The weight of each specimen is about 1 g. The conditions of the tests are put together in table 1.

Table 1 : Experimental conditions of the tests

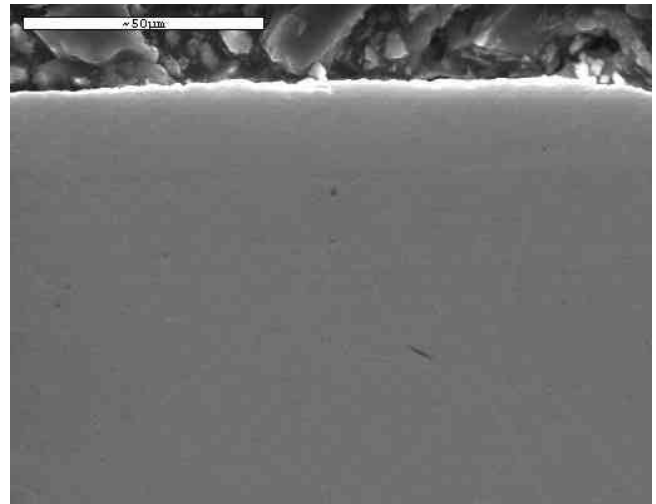
Test n°	Température (°C)	Duration (hour)	Pb-17Li mass (g)	W specimen	
				N°	mass (g)
1	800	3167	45.8	201	1.003760
2	1000	501	40.2	206	0.996126
3	1000	1110	43.0	203	0.998896
4	1000	982	47.1	205	0.997536

The test 3 performed at 1000°C for 1110 hours has not been used because at the end of the test, the molybdenum crucible had some cracks and some Pb-17Li has seeped out of it.

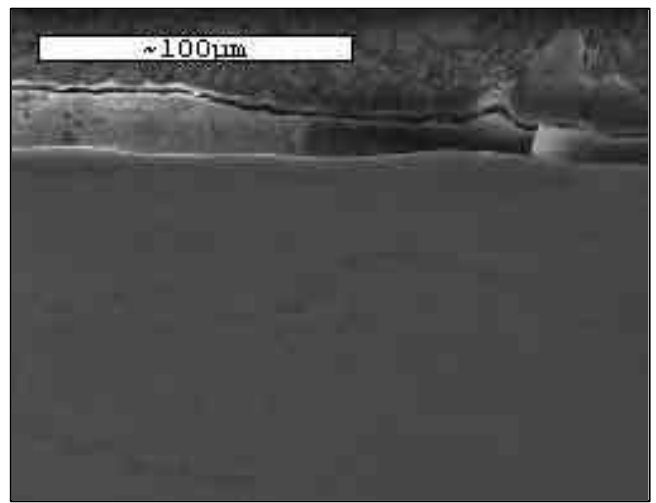
For the other tests, the chemical analyses of Pb-17Li by means of inductively coupled plasma mass spectroscopy (ICP-MS) indicate a tungsten content less than 5 wppm which correspond to the detection limit achievable by this technique.

Weight measurements of the tungsten specimens after the tests have not been performed because it has not been possible to remove Pb-17Li adhering to the specimens without damaging them.

Cross section micrographs of the specimens after the tests have been done and don't allow to see thickness decrease or corrosion (figure 2).



a)



b)

Figure 2 : SEM views of a specimen cross section:

a) before test

b) after 982 h in Pb-17Li at 1000°C

CONCLUSION

Tests have been performed in order to determine the tungsten solubility in Pb-17Li at 800°C and 1000°C. The experimental technique which has been used consists in immersing a tungsten specimen in a Pb-17Li bath for a long period and to measure the tungsten content in Pb-17Li at the end of the test.

Using this technique, very low tungsten solubility at 800°C and 1000°C in Pb-17Li have been observed (less than 5 wppm). These low values explain that no dissolution of tungsten in Pb-17Li at 800°C and 1000°C has been observed in the previous tests.

These values indicate that in a system at 1000°C maximum temperature the dissolution of tungsten even in flowing Pb-17Li and in the presence of thermal gradients should be very limited.

REFERENCES

- [1] F. BARBIER, F. HERBERT, Corrosion Behaviour of W alloy in static liquid Pb-17Li, CEA Report, RT-SCECF (November 2000).
- [2] T. DUFRENOY, T. DUFRENOY, V. LORENTZ, F. HERBERT, A. TERLAIN, Corrosion of tungsten by Pb-17Li, Rapport CEA RT-SCCME 595 (December 2001).

TASK LEADER

Thierry DUFRENOY

DEN/DPC/SCCME/LECNA
CEA Saclay
91191 Gif-sur-Yvette Cedex

Tél. : 33 1 69 08 16 16
Fax : 33 1 69 08 15 86

E-mail : thierry.dufrenoy@cea.fr

[illegible]

Task Title: COMPATIBILITY OF SiC_f/SiC COMPOSITES WITH LIQUID Pb-17Li

INTRODUCTION

Due to their high thermal conductivity, liquid metals and alloys are very efficient coolants. In the frame of fusion reactor development, the Pb-17Li eutectic alloy (17 at%Li) is the breeding and cooling candidate material for the self-cooled liquid metal breeding blanket (TAURO blanket) [1]. In this blanket concept, the SiC_f/SiC composite is proposed as the structural material. Moreover, with regard to the high heat flux components of fusion reactor, the Pb-17Li alloy is also considered to cool the divertor and SiC_f/SiC flow channel inserts (FCI) could be used as electrical insulators to avoid MHD pressure drops. It was already mentioned that brazing could be used to joint different complex parts of the blanket [2]. Some of the junctions cannot be obtained with current joining techniques such as welding, diffusion bonding and/or textile densification stage during the manufacture of the composite component. In this context, CEA-Grenoble is involved in the development of joining technologies for SiC_f/SiC composites using the BraSiC® process and of mechanical testing of the SiC_f/SiC junctions.

Corrosion tests of SiC_f/SiC composite Cerasep® N3-1 with isothermal static liquid Pb-17Li have already been performed at 800°C for 3000 h and 1000°C for 2500 h and no damages were observed [3,4]. No high temperature corrosion test of the BraSiC® H2 grade brazing alloy joining the SiC_f/SiC composites was performed and no data are available on the compatibility of BraSiC® alloy with liquid metals. In the frame of this task, it has therefore been performed a corrosion test on BraSiC® H2 grade brazing alloy in the presence of isothermal static liquid Pb-17Li at 800°C for 3000 h.

2002 ACTIVITIES

EXPERIMENTAL

An immersion test of a BraSiC® specimen in isothermal liquid Pb-17Li has been performed in a device schematically represented in figure 1. The device consists of various elements including an electric furnace, a alloy 601 container to protect the crucible from air oxidation during the test and a TZM (a molybdenum alloy) test crucible containing the specimen immersed in Pb-17Li. One thermocouple is located near the furnace resistors for the furnace temperature control and another is inside the alloy 601 container in a finger welded at its cover allowing the temperature measurement very near of the TZM crucible. It is the test temperature. The variations of this temperature during the test are less than 2 °C.

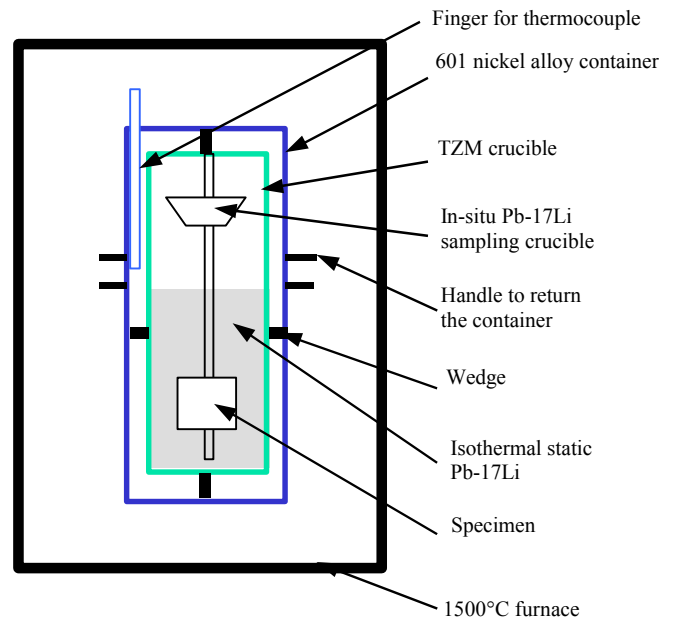


Figure 1 : Schematic drawing of the device

The TZM crucible ($\varnothing = 26$ mm, $H = 150$ mm) has a TZM holder welded to its cover. On this holder are fixed at the bottom the sample and at the top a little TZM crucible to in-situ sample some Pb-17Li by turning upside down the container with the crucible. This small Pb-17Li sample is used to perform a chemical analysis and determine the amount of dissolved elements. The advantages of this sampling system are: first the sample is no longer in contact with the specimen, second it is sufficiently small to be totally analysed and finally it avoids all the uncertainties induced by the presence of segregations when a frozen sample is only partially analysed.

All the operations to introduce the specimen in the crucible with the molten Pb-17Li were carried out in a glove box under a purified argon atmosphere. The Pb-17Li alloy was melted in a furnace and the liquid was poured into the crucible. About 600 g of Pb-17Li were introduced into the TZM crucible. One BraSiC® H2 grade brazing specimen was mounted onto the specimen holder, which was immersed into the molten alloy in the crucible. After cooling, the TZM crucible with the specimen was welded by electron beam technique. The as-sealed crucible was placed into the alloy 601 container which was subsequently electron beam welded.

The corrosion test was performed at 800 °C for 3000 h. At the end of the test, the container was turned upside down at 800 °C (in-situ sample Pb-17Li) and cooled. The container and the crucible were open. In the glove box, the Pb-17Li sample was recovered and the rest of Pb-17Li was melted to recover the BraSiC® H2 grade brazing specimen.

The BraSiC® H2 grade brazing alloy was manufactured and provided by the CEA-Grenoble. It was not possible to perform tests with SiC_f/SiC Cerasep® N3-1 with junctions of BraSiC® H2 grade brazing alloy because the SiC_f/SiC Cerasep® N3-1 is not available. Thus the BraSiC® H2 grade brazing alloy has been tested alone (20 x 20 x 15 mm³). The X-ray images of the surface of the as received BraSiC® H2 grade brazing show that it is mainly composed of rich Ti-V precipitates distributed in a Si rich matrix. The size and distribution of precipitates are not uniform.

RESULTS

Chemical analyses of the Pb-17Li alloy after test indicated 12 ± 2 ppm of Si, < 5 ppm of Ti, < 5 ppm of V. Taking into account the analysis uncertainties, these values are not far from those measured for Pb-17Li before test. Therefore, these results suggest that no or very small dissolution has occurred during the test perhaps due to a low Si, V solubilities in Pb-17Li.

On the other hand, analysis of the Pb-17Li alloy showed an increase in the molybdenum concentration: from less than 1 ppm before test, it increased to 30 ± 5 ppm after test. This indicates that a small dissolution of the TZM crucible has occurred during the test.

Geometrical measurements of the BraSiC® H2 grade brazing specimen performed before and after test with a micrometer gauge indicate no specimen dimension variations at least higher than a few tens of microns which is the uncertainty on this evaluation by our techniques. The specimen exposed to Pb-17Li was examined by SEM.

Figures 2 and 3 show a direct and a cross-section views of the specimen after the corrosion test. These figures show neither morphologic evolution nor chemical attack of the composite. No penetration of Pb-17Li can be seen: Pb-17Li is only adhering to the surface.

Therefore, in the tested conditions, no corrosion damage of the BraSiC® H2 grade brazing specimen has been observed

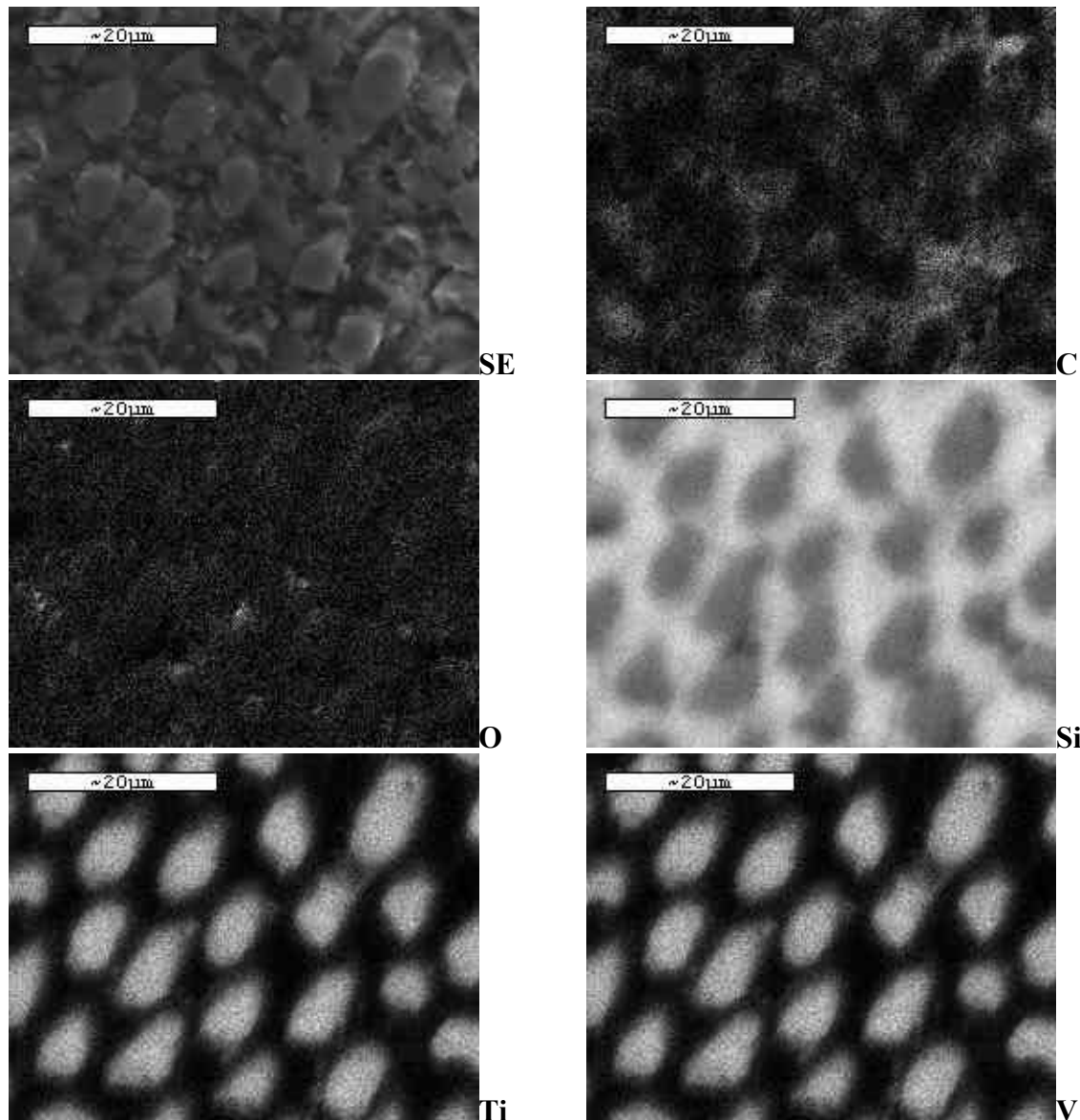


Figure 2 : X-ray images of the surface of the BraSiC® H2 grade brazing alloy specimen after 3000 h at 800°C in anisothermal static liquid Pb-17Li

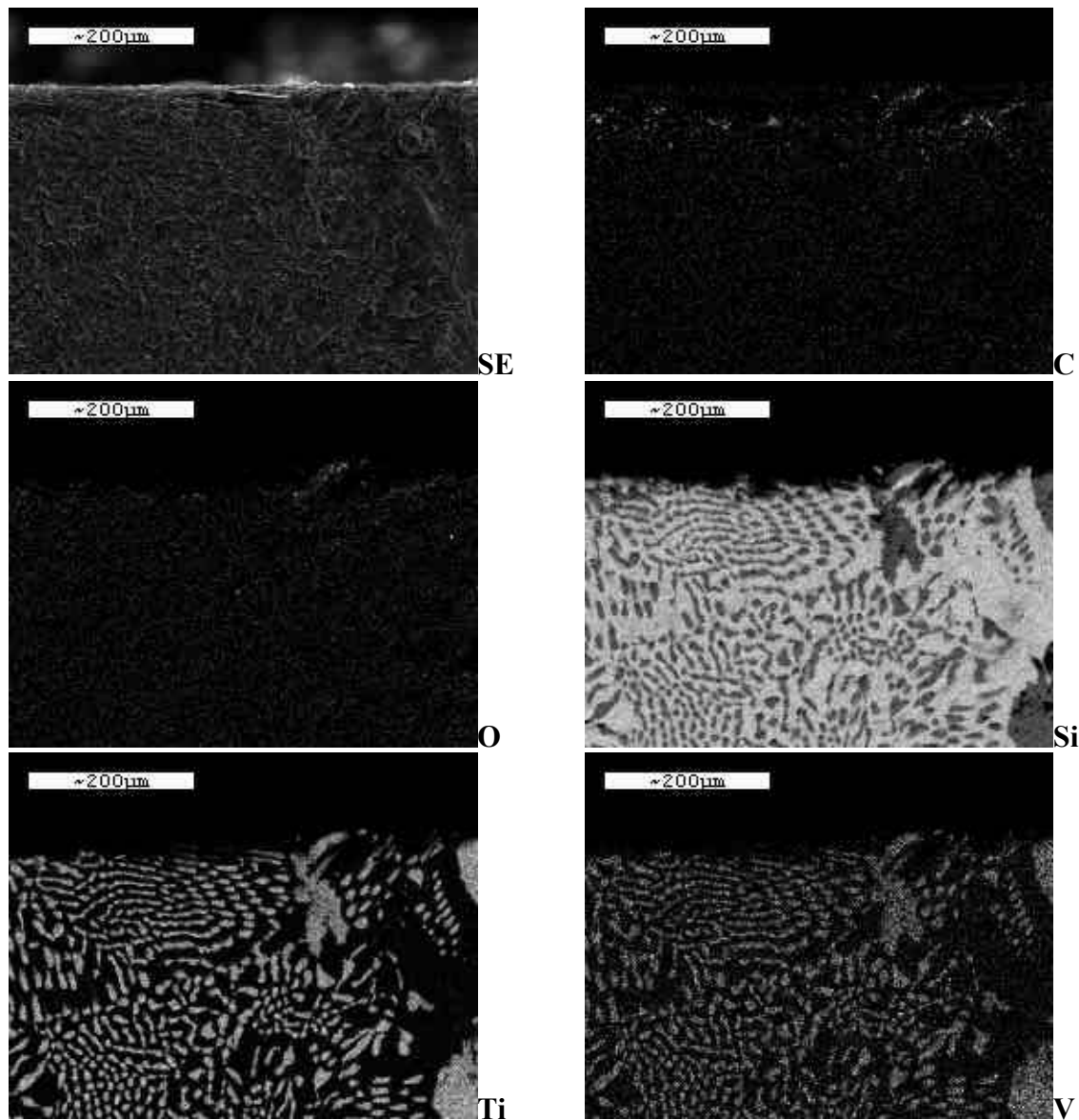


Figure 3 : X-ray images of the cross-section of the BraSiC® H2 grade brazing alloy specimen after 3000 h at 800°C in anisothermal static liquid Pb-17Li

CONCLUSION

The BraSiC® H2 grade brazing specimen was exposed to isothermal static liquid Pb-17Li at 800 °C up to 3000 h. The experiments indicate that the material has not reacted with the liquid alloy in these experimental conditions.

REFERENCES

- [1] L. Giancarli, J.P. Bonal, A. Caso, G. LE Marois, N.B. Morley and J.F. Salavy, Design requirements for SiC/SiC composite structural material in fusion power reactor blankets, Fus. Eng. & Des. 41 (1998).
- [2] G. Chaumat, A. Gasse, G. Coing-Boyat, G. Bourgeois, Long term program – Stage I. Development of joining techniques for the low activation materials (LAMs)

SiC-SiC composite, Note technique D.E.M./S.G.M. n°4/96, 9 janvier 1996.

- [3] F. Barbier, F. Herbert, Compatibility of SiC/SiC composite with static liquid Pb-17Li alloy CEA report, DTA/DEN/SCECF/LECNA/00-133 (November 2000).
- [4] Ph. Deloffre, A. Terlain, T. Dufrenoy, F. Herbert, V. Lorentz, Compatibility of SiC/SiC composite with liquid Pb-17Li alloy at high temperature, CEA report, DTA/DEN/SCCME/LECNA, RT-SCCME 586 (Décembre 2001).

REPORT

Ph. Deloffre, A. Terlain, F. Herbert, V. Chaumat, Compatibility of BraSiC® H2 grade brazing alloy with liquid Pb-17Li at 800 °C, CEA REPORT, RT 626 (JANUARY 2003).

TASK LEADER

Philippe DELOFFRE

DEN/DPC/SCCME/LECNA
CEA Saclay
91191 Gif-sur-Yvette Cedex

Tél : 33 1 69 08 16 18
Fax : 33 1 69 08 15 86

E-mail : deloffre.philippe@cea.fr

UT-TBM/MAT-LM/WET

Task Title: WETTING OF MATERIALS BY LIQUID METALS

INTRODUCTION

In fusion reactor, liquid metal cooling of High Heat Flux Components is considered for extracting heat fluxes. One possibility is to remove the heat by forced convection, employing relatively high velocity and insulating coatings on all channel walls or flow channel inserts.

In forced convection cooled liquid metal divertors, the Pb-Li alloy (17 at.% Li) has been selected because of its low reactivity with air and relatively low melting point.

Liquid metals are of interest but a major issue is the high temperature compatibility with the structural materials. As the running conditions of the systems under consideration are not yet well defined and costly to achieve in experimental devices, it is necessary to have some models taking into account the main corrosion factors.

Liquid metal corrosion manifests itself by various ways: dissolution, compound formation, liquid penetration and depends on various factors (temperature and thermal gradient, solid and liquid compositions, time, liquid metal velocity, surface state of the material..).

Corrosion studies are thus required for elucidate the corrosion mechanism and the main factors affecting it in order to make a material selection.

The wetting of solid materials by liquids is a determining factor in corrosion processes or when the liquid is involved in a heat transfer process (the wetting is necessary to an efficient heat removal).

When the corrosion process is studied and in particular the influence of the liquid velocity, it is fundamental to know the conditions of the specimen wetting to elaborate a model (incubation period due to wetting can leave to a bad interpretation of the results).

Therefore, it is of great importance to determine the conditions of wettability of a solid by a liquid.

A methodology to study the wetting of a solid by a liquid metal has previously been set up and applied to the Fe and Fe-7Cr and W /Pb and Pb-17Li systems. A synthesis of the results, focusing on the analysis of the influence on the initial surface state of the materials has been performed.

Moreover, a study of the penetration of Pb-17Li in SiC_f/SiC material which is an important phenomenon to characterise as a function of the surface state of the material (importance of the final coating on the composite, surface state after cutting...) has been carried out.

2002 ACTIVITIES

WETTING OF MATERIALS BY Pb-17Li

Wetting of tungsten by liquids Pb and Pb-17Li has been studied by means of the sessile drop and the dispensed drop techniques [1], [2]. The dispensed drop technique allows to break the natural oxide films which are present at the liquid and solid surfaces.

Different experiments have been previously performed with Fe (Armco grade), Fe-7Cr steel and tungsten as the substrate materials and Pb and Pb-17Li as the liquid metal or alloy. The main experimental results are presented in tables 1 and 2.

Table 1 : Contact angles, obtained by the set up drop technique, of liquid Pb and Pb-17Li on Fe and Fe-7Cr at 400°C under a 10⁻⁷ mbar vacuum

Liquid	Substrate			
	Fe	HT Fe ⁽¹⁾	Fe-7Cr	HT Fe-7Cr ⁽¹⁾
Pb	71°	45°-50°	90°	60°±3°
Pb-17Li	---	49°±1°	68°±2°	61°±3°

(1) Substrate with a in situ heat treatment at 800°C under vacuum just before the wetting test

Table 2 : Contact angles at 400°C under high vacuum of Pb and Pb-17Li drops on tungsten with (deoxidised) and without (oxidised) a first heat treatment at 900°C under high vacuum

Liquid	θ(deg)	
	W _{oxidised}	W _{desoxidised}
Pb	106 ± 2	67 ± 2
Pb-17Li	87 ± 2	49 ± 3*

The low difference between the contact angles obtained with Pb and Pb-17Li liquids on the heat treated Fe or Fe-7Cr shows that on these substrates the effect of Li on the wetting is low. On the other hand, the presence of Li increases the wettability of the Fe-7Cr substrate with its initial oxide layer: the contact angle is decreased by about 20° (table 1). This effect can be explained by the higher stability of the Li oxide compared to the iron oxides. Furthermore, Pb just as well Pb-17Li wet better the heat treated Fe (θ 45° to 50°) than Fe-7Cr (θ 60°): when the native oxide is at least removed on the material, the presence of Li in Pb has not a large influence on the wetting.

The reactivity between Fe and Pb is limited to a Mullins type grooving. At 800°C, the intergranular penetration depth after 20 minutes is about 200 nm and increases with time, following a $t^{1/3}$ law with the time. The reactivity between Fe and Pb-17Li in the sessile drop configuration is also mainly grooving at grain boundaries. The Fe-7Cr substrates undergo an intergranular corrosion but the grooves are not of Mullins type. Moreover, at 400°C, the grooves are hardly visible with a Scanning Electron Microscope ($d < 100$ nm).

The tungsten surface, heated directly at 400°C is not wetted by Pb (107° contact angle), whatever the atmosphere (high vacuum or an He+H₂ gas mixture). A non wetting / wetting transition is observed at 570°C in He+H₂ atmosphere and leads to a 60° contact angle value up to 800°C. After a high temperature heat treatment of tungsten under vacuum or He+H₂ atmosphere, the contact angle of Pb at 400°C is near 65°.

At 400°C, the addition of 17 at.% Li to Pb induces a contact angle decrease of 15° on tungsten with a prior high temperature heat treatment and of 20° without this heat treatment. When the tungsten surface is oxidised, this effect can be explained by the chemisorption of Li (Li has a very high affinity for oxygen) at the Pb/oxide film interface. When tungsten has been heat treated at high temperature in order to remove at least partially (some chemisorbed oxygen is always present at the surface) the native oxide layer, the θ variations could result from the local P_{O2} decrease at the triple line due to the $2\text{Li} + 1/2\text{O}_2 \rightarrow \text{Li}_2\text{O}$ chemical reaction. No reactivity between Pb (or Pb-17Li) and tungsten oxidised or not has been observed by means of SEM (0.1 μm resolution) even when the tungsten substrate has been heat treated at 900°C. As for Pb-17Li, and for long time experiences (several thousand seconds) a reaction has been observed outside the drop but near the triple line between Li and oxygen from the surface.

To have a good wetting of tungsten by Pb-17Li (contact angle characteristic of a liquid metal/solid metal contact) it is necessary to perform a preliminary heat treatment of tungsten at high temperature and under vacuum or an atmosphere with a very low oxygen activity. It is different from what it has been observed with Fe and Fe-7Cr: the Li activity in the Pb-17Li liquid is sufficient to modify or even suppress the native oxide film at the surface of these materials and therefore to insure a good wetting.

This study shows that it is very important to control the initial state of the substrate (presence of a native oxide or not) to have a good wetting by liquid lead. Concerning Pb-17Li, the presence of Li allows to destabilize the native oxide layer on Fe or Fe-7Cr steel but it is not the case for the tungsten material.

PENETRATION OF Pb-17Li IN SiC_f/SiC MATERIAL

The penetration of Pb-17Li in SiC_f/SiC material has been studied by performing an immersion test at 1000°C for 2500 h of machined SiC_f/SiC material in Pb-17Li at high temperature.

Figure 1 shows a schematic view of the experimental device. The material which has been used is the 3 dimensional composite Cerasep[®] N3-1.

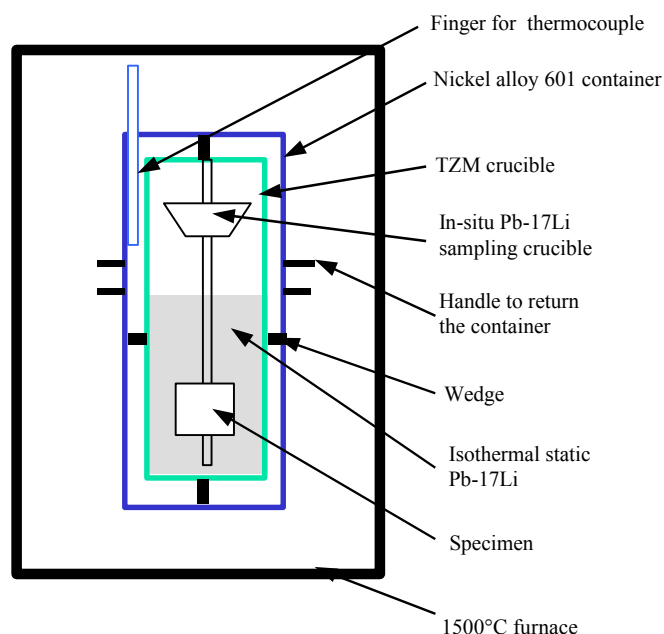


Figure 1 : Schematic view of the experimental device

It is made of SiC fibres (Nicalon NL207) produced by Nippon Carbon and densified by chemical vapour infiltration process (CVI) and covered by a superficial layer. Three specimens have been machined from plate as it is shown in figure 2.

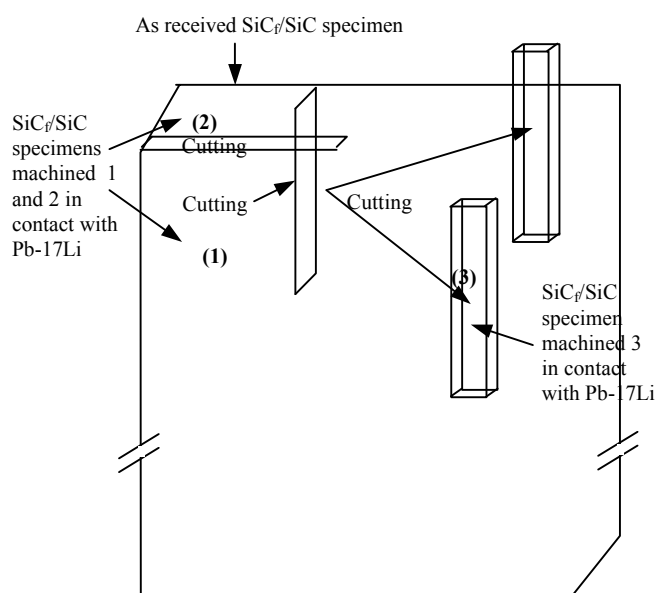
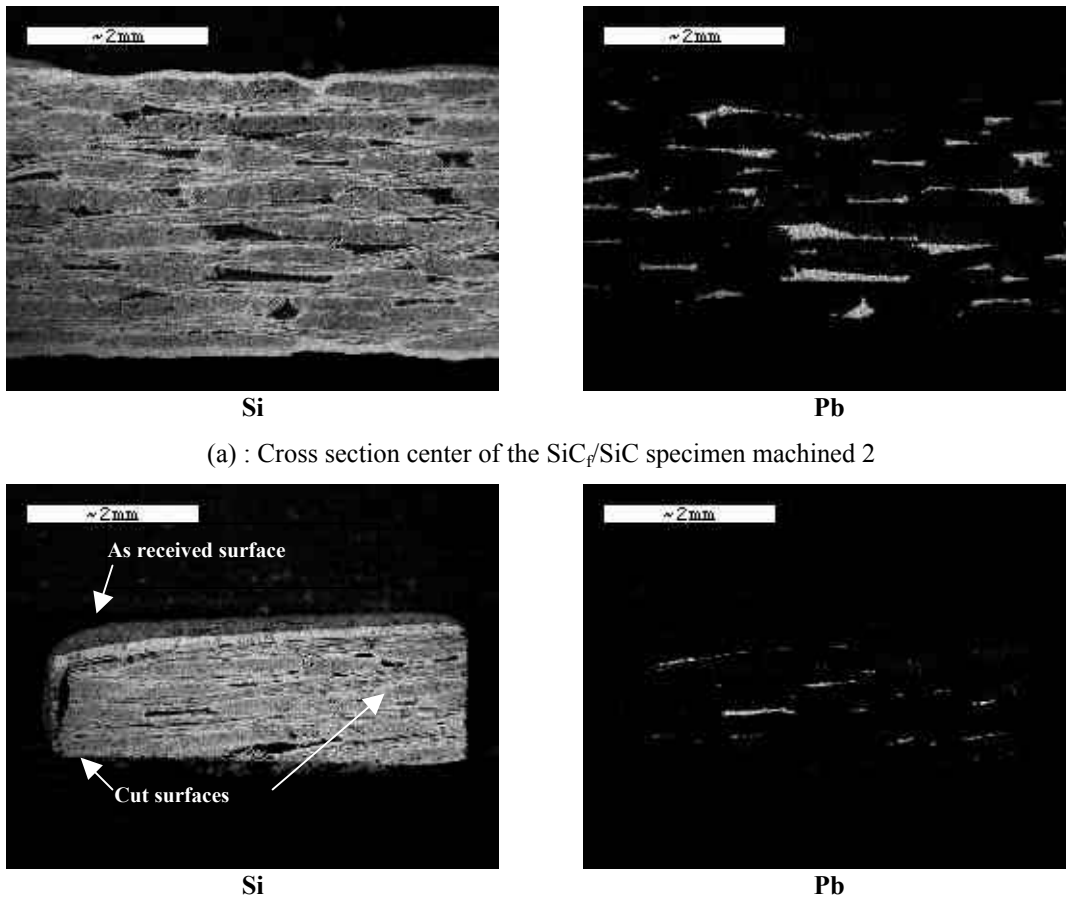


Figure 2 : SiC_f/SiC specimens machined before contact with Pb-17Li

After the test, cross section micrographs have been made and EDS analyses has been performed in order to evaluate the penetration of Pb-17Li inside the material. Figure 3 shows some views of the specimens after the test. We can see that Pb-17Li has penetrated in all the porosities and in all the thickness of the specimen.



(a) : Cross section center of the SiC_f/SiC specimen machined 2

(b) : Cross section center of the SiC_f/SiC specimen machined 3

Figure 3 : Cross sections x-ray images of the SiC_f/SiC specimens machined 2 and 3 after 2500 h at 1000°C in isothermal static liquid Pb-17Li

This test shows that without the final coating, large penetrations of Pb-17Li occur in this material and probably can modify its mechanical properties and favour a decohesion of the fibres.

CONCLUSION

This study shows that it is very important to control the initial state of the substrate (presence of a native oxide or not) to have a good wetting by liquid lead. Concerning Pb-17Li, the presence of Li allows to destabilize the native oxide layer on Fe or Fe-7Cr steel but it is not the case for the tungsten material.

Otherwise, it has been observed that large penetrations of Pb-17Li in SiC_f/SiC occur when the coating on this material is removed.

REFERENCES

- [1] P. PROTSENKO, N. EUSTATHOPOULOS, A. TERLAIN, Wetting of materials by liquid lead, CEA Report, RT SCECF 518 (November 1999).

- [2] P. PROTSENKO, M. JEYMOND, N. EUSTATHOPOULOS, A. TERLAIN, Wetting and reactivity in the Pb-17Li/Fe and Pb-17Li/Fe-7Cr systems, CEA Report, RT SCECF 550 (November 2000).

REPORT

A. Terlain, Ph. Deloffre, F. Herbert, Wetting and penetration of materials by Pb or Pb-17Li, CEA Report, to be issued.

TASK LEADER

Anne TERLAIN

DEN/DPC/SCCME/LECNA
CEA Saclay
91191 Gif-sur-Yvette Cedex

Tél. : 33 1 69 08 16 18
Fax : 33 1 69 08 15 86

E-mail : anne.terlain@cea.fr